Voltage and current density in a rectangle with point in- and ejection via Green's functions and q-analysis

P. Van Mieghem*

Delft University of Technology
25 June 2026

Abstract

The current density in a rectangle in the $D = 2$ dimensional Euclidean space, where opposite point charges are placed in a source s and a destination d, is computed as the gradient of a potential that obeys the Poisson equation (first law of Maxwell). Although the computation of the current density in a 2D rectangle is a classical problem, several barriers (e.g. very slow convergence of double Fourier series) were eventually alleviated by a q-analysis, related to Gaussian polynomials and Jacobi's theta-functions, that form the basic building blocks for any elliptic function. We present an exact and computationally very efficient analytic formula of the potential and the magnitude of the current density in a rectangle.

1 Introduction

We compute the potential and current density in each point of a rectangle in the two-dimensional Euclidean space, where at the source point s a unit current is injected, which leaves the rectangle at the destination point d. The electric unit current thus spreads from the injection point s to the ejection point d over the entire rectangle, steered by the first law of Maxwell, briefly reviewed in Section 2. Although the potential and current computation is a classical problem, that is usually solved by Fourier series, our main result is the Green's function (24) in terms of a q-function (25), which belongs to the class of elliptic functions. A famous earlier victory in physics is the *phenomenal* paper [1] of Noble-Prize winner Ralph Onsager, in which he solved the 2D Ising model *exactly* using elliptic functions (Jacobi theta functions, Jacobian elliptic functions and elliptic integrals [1, from p. 144 on]).

Our motivation arose from Kitsak *et al.* [2], who conjectured that the shortest path $\mathcal{P}^*_{sd}$ in many graphs, where only partial information of the graph and its link weights is available as in most real-world networks, is close to the geodesic from s to d. The knowledge of the set of network nodes that most likely lie on the shortest path between a source and destination is important, both for the network operator to secure and for the adversary to eliminate or disrupt those nodes. A simple example of a partially known graph is the hard random geometric graphs (HRGG), in which N

*Faculty of Electrical Engineering, Mathematics and Computer Science, P.O Box 5031, 2600 GA Delft, The Netherlands; *email*: P.F.A.VanMieghem@tudelft.nl

nodes are uniformly distributed in a 2D rectangle and connected to other nodes that lie within a given distance r_0. Randomness here reflects our uncertainty about the precise nodal positions in a partially observed network. Random geometric graphs (RGGs) have been studied extensively (see e.g. references in [3],[2]). RGGs can model transportation networks such as wireless and airline networks as well as infrastructural networks like power grids. RGGs can be applied to analyze the structure of large data sets and in modelling ad hoc networks (such as vehicular, disaster relief, sensor and flying swarm robotics networks). The probability that a point (x, y) in the rectangle belongs to the shortest path $\mathcal{P}_{sd}^*$ between a given pair (s, d) of nodes in the HRGG is difficult to compute analytically, while the current density and the electric potential in a continuous space can be computed as shown below. In the high-density limit ($N \to \infty$) of an HRGG with link connectivity distance $r_0 = O\left(\frac{1}{\sqrt{N}}\right)$, we conjecture that the magnitude of current density $|j(x, y)|$ in each point (x, y) of the rectangle, due to current in- and ejection at s and d, is proportional to the probability that the point (x, y) lies on the shortest path $\mathcal{P}_{sd}^*$ in an HRGG between source s and drain d.

The paper presents an exploratory journey from Fourier series towards q-functions, belonging to the class of elliptic functions. The paper starts in Section 3 by computing the Laplacian equation (1) in 3D for the current in- and ejection in the beam in Fig. 1. Although the computation is rather involved, but a standard exercise in solving the Laplacian equation in rectangular or Cartesian coordinates, the importance is that an exact solution of the potential[1] $V(x, y, z) + V_{\text{ref}}$ exists, which is written as a double Fourier series in (10). Section 4 considers the limit where the size c of the parallellepipidum in Fig. 1 tends to zero, thus forming a rectangle in the xy-plane with sizes a and b. Here, we encounter physical limitations, because the injection current is orthogonal to the xy-plane and thus, there are no vector components in the x and y-directions, which complicates the limit $c \to 0$ in our setting! Nevertheless, we show that we can continue due to the mathematical beauty of a renormalization argument and Green's function theory. First, we present a double Fourier series for the potential or voltage $V(x, y, 0)$ in (12) and show agreement with the corresponding Green's function. However, the double Fourier series of the current density converges very slowly, which motivated the computation of a single Fourier series, presented in Section 4.2. Although the single Fourier is computationally far superior than the double Fourier series, inaccuracies at x- and y-lines passing through injection point s and ejection point d, explained in Section 4.3, have motivated the analytic evaluation of the single Fourier series (20) and (22). Surprisingly, perhaps, our analysis leads to the product $(a; q)_n = \prod_{k=0}^{n-1} \left(1 - aq^k\right)$, which is a basic product in q-analysis, briefly reviewed in Appendix G on Gaussian polynomials. The product $(a; q)_n$ also appears in Jacobi's theta functions. Apart from this connection to elliptic functions, the resulting series for the current density converges extremely fast, at least in a square $a = b$, to the extent that only 1 term seems[2] accurate enough in plots.

In the many Appendices, we have positioned important knowledge, that wanders around the direct path from the Fourier analysis towards the q-analysis. A brief review of Green's function theory (Appendix B), of q-analysis (Appendix F) and of Gaussian polynomials (Appendix G) as well

[1] The potential $V(x, y, z)$ is only unique if a reference potential V_{ref} is chosen.

[2] There is no visual difference between the current density (computed in Fig. 4) with only 1 term compared to the series with more than one term, due to an expansion in powers of $e^{-2\pi} \approx \frac{1}{535}$. The same amazing convergence appears in Jacobi theta series.

as tedious computations are placed in the Appendices. The effective resistance matrix of a graph, containing the effective resistance ω_{ij} between all pairs (i,j) of nodes, is an important graph matrix, as illustrated in [4, Chapter 5], whose theory is built upon Kirchoff's circuit laws and the law of Ohm and which is intimately related to the simplex geometry [5] of any graph. The effective resistance ω_{ij} lower bounds the weight [4, Sec. 5.7] (i.e. hopcount, the number of links in a path, in an unweighted graph) of a shortest path $\mathcal{P}_{ij}^*$. The rather straightforward applications of the theory, with explicit formulae for the voltage in 2D and 3D, is shown to lead to surprises in Appendix E.

2 The flow of electrical current

The first law of Maxwell [6] is Gauss's law,

$$\oint_A \overrightarrow{E}.\overrightarrow{dS} = \frac{1}{\epsilon_0}\iiint_v \rho dr$$

which states that the electric flux, which is the scalar product of the electric field $\overrightarrow{E}$ and the orthogonal vector $\overrightarrow{dS}$ on the surface, through a closed surface A that surrounds a region with volume v equals the total amount of charges, specified by the charge density $\rho(x,y,z)$ at each point (x,y,z), that are contained in that region with volume v, divided by the permittivity ϵ_0 in vacuum. The permittivity in vacuum is a constant and equal to $\epsilon_0 = 8.85\ 10^{-12} C^2/Nm^2$. The differential form of Maxwell's first law is

$$\text{div}\ \overrightarrow{E} = \frac{1}{\epsilon_0}\rho$$

The electric field is defined as $\overrightarrow{E} = -\,\text{grad}\, V$, where the potential V is specified by the Poisson equation,

$$\Delta V = -\frac{1}{\epsilon_0}\rho$$

that follows from Maxwell's first law $\text{div}\ \overrightarrow{E} = \frac{1}{\epsilon_0}\rho$ as $\text{div}\,\text{grad}\, V = -\frac{1}{\epsilon_0}\rho$, where

$$\text{div}\,\text{grad}\, V = \Delta V = \frac{\partial^2 V}{\partial x^2} + \frac{\partial^2 V}{\partial y^2} + \frac{\partial^2 V}{\partial z^2}$$

and the potential $V(x,y,z)$ is expressed in Cartesian coordinates. The differential operator $\Delta = \frac{\partial^2}{\partial x^2} + \frac{\partial^2}{\partial y^2} + \frac{\partial^2}{\partial z^2}$ is called the Laplacian, which is a continuous limit of the discrete Laplacian matrix Q of a graph [4].

A beam in Fig. 1 is a representation in three spacial dimensions, defined by the Cartesian coordinate frame with x-axis, y-axis and z-axis. The current injection is orthogonal to the xy-plane, i.e. $z = 0$. Fig. 1 illustrates a beam or parallellepipidum with size a, b, c of a certain material with constant resistivity ϱ. A unit current is injected in a source point s in the $z = 0$-plane at coordinates $(x_{in}, y_{in}, 0)$. The current leaves the beam at the drain point d at $(x_{out}, y_{out}, 0)$. Both injection and ejection point lie at the surface of the beam. Here, the injection point s and ejection point d lie in the same xy-plane. However, the drain point d can also be placed on any other surface plane of the beam, i.e. at $y = 0$ or $y = b$, at $x = 0$ or $x = a$ and at $z = 0$ or $z = c$.

We compute the potential $V(x,y,z)$ at a point (x,y,z) inside and on the surface of the beam. Since no charges are contained inside the beam, the Poisson equation reduces to the Laplacian partial

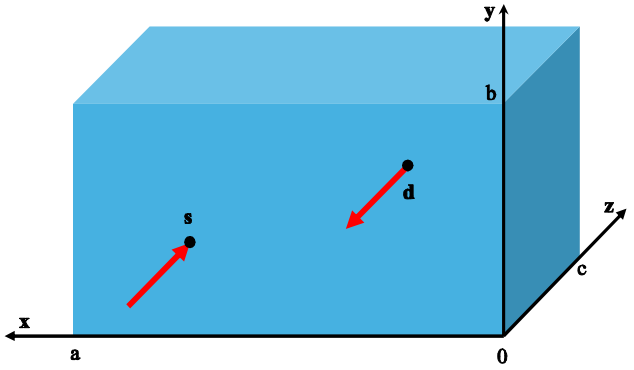


Figure 1: The coordinate axes in a parallellepipidum, in which a current is injected at the source point s and ejected at the drain point d.

differential equation

$$\frac{\partial^2 V}{\partial x^2} + \frac{\partial^2 V}{\partial y^2} + \frac{\partial^2 V}{\partial z^2} = 0 \tag{1}$$

with boundary conditions $\frac{\partial V}{\partial x} = 0$ at $x = 0$ and $x = a$, $\frac{\partial V}{\partial y} = 0$ at $y = 0$ and $y = b$ and $\frac{\partial V}{\partial z} = 0$ at $z = c$, implying that no current[3] $\overrightarrow{j}(x, y, z) = -\sigma \overrightarrow{E} = -\sigma \operatorname{grad} V$ can flow through the surface of the beam, except at the plane $z = 0$. The current, orthogonal to the xy-plane and equal to $\frac{\partial V}{\partial z} = -\frac{1}{\sigma} I = -\varrho I$, is injected at the source point $s = (x_{in}, y_{in}, 0)$ and that same current $\frac{\partial V}{\partial z} = \varrho I$ is leaving at the drain point $d = (x_{out}, y_{out}, 0)$ in the other direction. The law of Ohm then states that the corresponding resistance equals $R_{sd} = \frac{V(x_{in}, y_{in}, 0) - V(x_{out}, y_{out}, 0)}{I}$.

3 Solution of the Laplacian in 3D

3.1 Separation of dimensions

We employ the standard method of separation of dimensions and assume that a solution of the form $V(x, y, z) = X(x) Y(y) Z(z)$ exists. The Laplacian (1) then reduces to

$$X''(x) Y(y) Z(z) + X(x) Y''(y) Z(z) + X(x) Y(y) Z''(z) = 0$$

[3] The current density is a vector $\overrightarrow{j}(x, y, z) = j_x(x, y, z) \overrightarrow{e}_x + j_y(x, y, z) \overrightarrow{e}_y + j_z(x, y, z) \overrightarrow{e}_z$, written by the arrow above the symbol and $\overrightarrow{e}_i$ is the basic, unit norm vector in direction i, orthogonal to any other direction. The magnitude $\left|\overrightarrow{j}(x, y, z)\right|$ of the current density is a vector norm, for which we employ here the simplest possible form of a scalar product $\left|\overrightarrow{j}(x, y, z)\right|^2 = \overrightarrow{j}(x, y, z) . \overrightarrow{j}(x, y, z)$. Sometimes, we omit the arrow when talking about the magnitude $|j(x, y, z)|$ of the current density. The current density through a surface A in the z-direction of the beam is $I = \int_A j_z(x, y, 0)\, dxdy$. Hence, if $j_z(x, y, 0) = j$ in a point can be regarded as constant and the same for all points of the surface, then the current through that surface is $I = jA$. The resistivity $\varrho = \sigma^{-1}$ has units $[\Omega m]$, i.e. Ohm meter, whereas the conductivity σ is expressed in $[S/m]$, i.e. Siemens per meter.

where $f''(x) = \frac{d^2 f}{dx^2}$. Dividing[4] by $V(x,y,z)$,

$$\frac{X''(x)}{X(x)} + \frac{Y''(y)}{Y(y)} + \frac{Z''(z)}{Z(z)} = 0 \tag{2}$$

and differentiating with respect to x, y and z shows that

$$\begin{cases} \frac{d}{dx}\left(\frac{X''(x)}{X(x)}\right) = 0 \\ \frac{d}{dy}\left(\frac{Y''(y)}{Y(y)}\right) = 0 \\ \frac{d}{dz}\left(\frac{Z''(z)}{Z(z)}\right) = 0 \end{cases}$$

Integration then gives

$$\begin{cases} \frac{X''(x)}{X(x)} = \lambda_x \\ \frac{Y''(y)}{Y(y)} = \lambda_y \\ \frac{Z''(z)}{Z(z)} = \lambda_z \end{cases} \tag{3}$$

while substitution into (2) indicates that the constants of integration must satisfy

$$\lambda_x + \lambda_y + \lambda_z = 0 \tag{4}$$

Since the potential $V(x,y,z)$ is a real function in the spacial coordinates x, y and z, the integration or separation constants λ_x, λ_y and λ_z in (3) are real.

In summary, the separation of dimensions has reduced the partial differential equation into three linear second-order differential equations in one variable in (3) of the form

$$W''(w) - \lambda_w W(w) = 0$$

whose general solution for $\lambda_w \neq 0$ and constants $\widetilde{A}, \widetilde{B}$ is

$$W(w) = \widetilde{A} e^{-\sqrt{\lambda_w} w} + \widetilde{B} e^{\sqrt{\lambda_w} w}$$

but if $\lambda_w = -|\lambda_w| = i^2 |\lambda_w|$,

$$W(w) = A \sin\sqrt{|\lambda_w|} w + B \cos\sqrt{|\lambda_w|} w$$

If $\lambda_w = 0$, then $W(w) = \alpha w + \beta$, for real constants α and β.

3.2 Introduction of boundary conditions

The next step is to incorporate the boundary conditions, $\frac{\partial V}{\partial x} = 0$ at $x = 0$ and $x = a$, $\frac{\partial V}{\partial y} = 0$ at $y = 0$ and $y = b$ and $\frac{\partial V}{\partial z} = 0$ at $z = c$, that translate to

$$\begin{cases} X'(0) = X'(a) = 0 \\ Y'(0) = Y'(b) = 0 \\ Z'(c) = 0 \end{cases} \tag{5}$$

[4] We can always choose a reference potential in such a way that $V(x,y,z) \neq 0$ at any point $p = (x,y,z)$ inside and on the beam.

For the x-dimension with general solution $X(x) = A_X \sin\sqrt{|\lambda_x|}x + B_X \cos\sqrt{|\lambda_x|}x$ for $\lambda_x \neq 0$, it holds that

$$X'(x) = A_X\sqrt{|\lambda_x|}\cos\sqrt{|\lambda_x|}x - B_X\sqrt{|\lambda_x|}\sin\sqrt{|\lambda_x|}x$$

Requiring that $X'(0) = 0$ leads to $X'(0) = A_X\sqrt{|\lambda_x|} = 0$, while the other boundary condition $X'(a) = 0$ implies that $-B_X\sqrt{|\lambda_x|}\sin\sqrt{|\lambda_x|}a = 0$. The condition $\sin\sqrt{|\lambda_x|}a = 0$ is met, when $\sqrt{|\lambda_x|}a = k\pi$, i.e. $\sqrt{|\lambda_x|} = \frac{k\pi}{a}$ for $k \in \mathbb{N}_0$. If $\lambda_x = 0$, then the solution is $X(x) = \alpha x + \beta$ and $X'(x) = \alpha$. The boundary condition $X'(0) = 0$ requires that $\alpha = 0$, in which case $X'(x) = 0$ for all real x so that the boundary condition $X'(a) = 0$ is also satisfied.

Combining all shows that

$$X(x) = B_X \cos\left(\frac{k\pi}{a}x\right)$$

for all non-negative integers k, i.e. $k = 0, 1, 2, \ldots$. Similarly, for the y-dimension, we find that $Y(y) = B_Y \cos\frac{l\pi}{b}y$. Also, the integration or separation constants $|\lambda_x| = \left(\frac{k\pi}{a}\right)^2$ and $|\lambda_y| = \left(\frac{l\pi}{b}\right)^2$ are non-negative and both $k, l \in \mathbb{N}$.

The remaining z-dimension is a little different. Since $\lambda_z = -\lambda_x - \lambda_y$ by (4) and the boundary problem requires that $\lambda_x = -|\lambda_x| = -\left(\frac{k\pi}{a}\right)^2$ and $\lambda_y = -|\lambda_y| = -\left(\frac{l\pi}{b}\right)^2$, the corresponding differential equation $Z''(z) - \lambda_z Z(z) = 0$ in (3) with $\lambda_z = \left(\frac{k\pi}{a}\right)^2 + \left(\frac{l\pi}{b}\right)^2 \geq 0$ has the solution

$$Z(z) = \widetilde{A}_Z e^{-\sqrt{\lambda_z}z} + \widetilde{B}_Z e^{\sqrt{\lambda_z}z}$$

and

$$Z'(z) = \sqrt{\lambda_z}\left(-\widetilde{A}_Z e^{-\sqrt{\lambda_z}z} + \widetilde{B}_Z e^{\sqrt{\lambda_z}z}\right)$$

The boundary condition $Z'(c) = 0$ translates to $\widetilde{B}_Z = \widetilde{A}_Z e^{-2\sqrt{\lambda_z}c}$. Hence,

$$\begin{aligned} Z(z) &= \widetilde{A}_Z\left(e^{-\sqrt{\lambda_z}z} + e^{\sqrt{\lambda_z}(z-2c)}\right) = \widetilde{A}_Z e^{-\sqrt{\lambda_z}c}\left(e^{-\sqrt{\lambda_z}(z-c)} + e^{\sqrt{\lambda_z}(z-c)}\right) \\ &= 2\widetilde{A}_Z e^{-\sqrt{\lambda_z}c}\cosh\left(\sqrt{\lambda_z}(z-c)\right) \end{aligned}$$

Writing for the unknown coefficient $B_Z = 2\widetilde{A}_Z e^{-\sqrt{\lambda_z}c}$, the solution in z-dimension is

$$Z(z) = B_Z \cosh\left(\sqrt{\left(\frac{k\pi}{a}\right)^2 + \left(\frac{l\pi}{b}\right)^2}(z-c)\right)$$

In summary, a particular solution for the potential of the Laplace equation (1), subject to the boundary conditions (5), is

$$V(x,y,z) = X(x)Y(y)Z(z) = B_X B_Y B_Z \cos\left(\frac{k\pi}{a}x\right)\cos\left(\frac{l\pi}{b}y\right)\cosh\left(\sqrt{\left(\frac{k\pi}{a}\right)^2 + \left(\frac{l\pi}{b}\right)^2}(z-c)\right)$$

where the integers $k, l \in \mathbb{N}$ and the coefficients B_X, B_Y and B_Z are constants, independent of the spacial coordinates x, y and z.

3.3 General solution of the Laplacian differential equation

Since the Laplacian differential equation is a linear equation, any particular solution for a pair of integers (k,l) is also a solution, as well as any linear combination of them. The most general solution is then

$$V(x,y,z)=\sum_{k=0}^{\infty}\sum_{l=0}^{\infty}\varphi_{kl}\cos\frac{k\pi}{a}x\cos\frac{l\pi}{b}y\cosh\left(\sqrt{\left(\frac{k\pi}{a}\right)^2+\left(\frac{l\pi}{b}\right)^2}(z-c)\right) \tag{6}$$

This general solution of the voltage in $D=3$ dimensions can be extended to a D-dimensional Euclidean space, where the D-rectangle has sizes $a_1,a_2,\ldots,a_D$, as

$$V(x_1,x_2,\ldots,x_D)=\sum_{k_1=0}^{\infty}\sum_{k_2=0}^{\infty}\cdots\sum_{k_{D-1}=0}^{\infty}\varphi(k_1,\ldots,k_{D-1})\prod_{j=1}^{D-1}\cos\left(\frac{k_j\pi}{a_j}x_j\right)\cosh\left(\sqrt{\sum_{j=1}^{D-1}\left(\frac{k_j\pi}{a_j}\right)^2}(x_D-a_D)\right) \tag{7}$$

The coefficient function $\varphi(k_1,\ldots,k_{D-1})$ must be determined from the current injection and -ejection. The boundary conditions that no current can flow through any face of the D-rectangle, except for one face containing the injection and ejection points, are satisfied. We proceed with the $D=3$ Euclidean case further.

It remains to determine the coefficients φ_{kl} in (6) so that the two remaining current-injection conditions, $\frac{\partial V}{\partial z}=\varrho I$ at the source point $s=(x_{in},y_{in},0)$ and $\frac{\partial V}{\partial z}=-\varrho I$ at the drain point $d=(x_{out},y_{out},0)$, are satisfied,

$$\frac{\partial V(x,y,0)}{\partial z}=\varrho I\left(\delta(x-x_{in},y-y_{in},0)-\delta(x-x_{out},y-y_{out},0)\right)$$

where the Dirac delta function $\delta(x)$ underlines "point" in- and ejection of the current.

The derivative

$$\frac{\partial V}{\partial z}=\sum_{k=0}^{\infty}\sum_{l=0}^{\infty}\sqrt{\left(\frac{k\pi}{a}\right)^2+\left(\frac{l\pi}{b}\right)^2}\varphi_{kl}\cos\frac{k\pi}{a}x\cos\frac{l\pi}{b}y\sinh\left(\sqrt{\left(\frac{k\pi}{a}\right)^2+\left(\frac{l\pi}{b}\right)^2}(z-c)\right) \tag{8}$$

at the source s and drain d is

$$\begin{aligned}\left.\frac{\partial V}{\partial z}\right|_{s=(x_{in},y_{in},0)}&=\sum_{k=0}^{\infty}\sum_{l=0}^{\infty}\sqrt{\left(\frac{k\pi}{a}\right)^2+\left(\frac{l\pi}{b}\right)^2}\varphi_{kl}\cos\frac{k\pi}{a}x_{in}\cos\frac{l\pi}{b}y_{in}\sinh\left(\sqrt{\left(\frac{k\pi}{a}\right)^2+\left(\frac{l\pi}{b}\right)^2}c\right)\\&=\varrho I\delta(x-x_{in},y-y_{in},0)\\\left.\frac{\partial V}{\partial z}\right|_{d=(x_{out},y_{out},0)}&=\sum_{k=0}^{\infty}\sum_{l=0}^{\infty}\sqrt{\left(\frac{k\pi}{a}\right)^2+\left(\frac{l\pi}{b}\right)^2}\varphi_{kl}\cos\frac{k\pi}{a}x_{out}\cos\frac{l\pi}{b}y_{out}\sinh\left(\sqrt{\left(\frac{k\pi}{a}\right)^2+\left(\frac{l\pi}{b}\right)^2}c\right)\\&=-\varrho I\delta(x-x_{out},y-y_{out},0)\end{aligned}$$

while $\left.\frac{\partial V}{\partial z}\right|_u=0$ at any other point $u=(x,y,0)$.

3.4 Current injection in the plane $z=0$

After letting

$$\psi_{kl}=\varphi_{kl}\sqrt{\left(\frac{k\pi}{a}\right)^2+\left(\frac{l\pi}{b}\right)^2}\sinh\left(c\sqrt{\left(\frac{k\pi}{a}\right)^2+\left(\frac{l\pi}{b}\right)^2}\right)$$

we will reformulate the current injection $j_z = \sigma \frac{\partial V}{\partial z}$ in the plane $z = 0$ in (8) more generally as

$$\left.\frac{\partial V}{\partial z}\right|_{z=0} = \sum_{k=0}^{\infty}\sum_{l=0}^{\infty} \psi_{kl} \cos\frac{k\pi}{a}x \cos\frac{l\pi}{b}y = g\left(x,y\right)$$

The goal is to express the coefficients ψ_{kl} in terms of the boundary current in- and ejection function $g\left(x,y\right)$.

Multiplying both sides with $\cos\frac{k'\pi}{a}x \cos\frac{l'\pi}{b}y$,

$$g\left(x,y\right)\cos\frac{k'\pi}{a}x \cos\frac{l'\pi}{b}y = \sum_{k=0}^{\infty}\sum_{l=0}^{\infty} \psi_{kl} \cos\frac{k'\pi}{a}x \cos\frac{k\pi}{a}x \cos\frac{l\pi}{b}y \cos\frac{l'\pi}{b}y$$

Integrating x from 0 to a and y from 0 to b,

$$\int_0^a dx \int_0^b dy\; g\left(x,y\right)\cos\frac{k'\pi}{a}\cos\frac{l'\pi}{b}y = \sum_{k=0}^{\infty}\sum_{l=0}^{\infty} \psi_{kl}\left(\int_0^a \cos\frac{k'\pi}{a}x\cos\frac{k\pi}{a}xdx\right)\left(\int_0^b \cos\frac{l\pi}{b}y\cos\frac{l'\pi}{b}y\right)$$

invoking the orthogonality relations $\int_0^a \cos\frac{k'\pi}{a}x\cos\frac{k\pi}{a}xdx = \frac{a}{\pi}\int_0^\pi \cos k'\theta\cos k\theta d\theta = a\left(1_{\{k=0\}} + \frac{1}{2}1_{\{k\neq 0\}}\right)\delta_{k'k}$, leads to

$$\psi_{k'l'} = \begin{cases} \frac{4}{ab}\int_0^a dx \int_0^b dy\; g\left(x,y\right)\cos\frac{k'\pi}{a}\cos\frac{l'\pi}{b}y & \text{for } k'>0 \text{ and } l'>0 \\ \frac{2}{ab}\int_0^a dx \int_0^b dy\; g\left(x,y\right)\cos\frac{k'\pi}{a}\cos\frac{l'\pi}{b}y & \begin{cases}\text{for } k'=0 \text{ and } l'>0\\ \text{or } k'>0 \text{ and } l'=0\end{cases} \\ \frac{1}{ab}\int_0^a dx \int_0^b dy\; g\left(x,y\right) & \text{for } k'=0 \text{ and } l'=0 \end{cases} \tag{9}$$

In our setting, we must choose the function $g\left(x,y\right)$ to satisfy the current injection at the source point $s = (x_{in}, y_{in})$ and the current ejection at the drain point $d = (x_{out}, y_{out})$,

$$g\left(x,y\right) = \varrho I\left\{\delta\left(x-x_{in}\right)\delta\left(y-y_{in}\right) - \delta\left(x-x_{out}\right)\delta\left(y-y_{out}\right)\right\}$$

Hence, the double integral in $\psi_{k'l'}$ becomes, with $c_{k'l'}$ representing the three different conditions for k' and l',

$$\begin{aligned}\psi_{k'l'} &= \frac{\rho I c_{k'l'}}{ab}\int_0^a dx \int_0^b dy\left(\delta\left(x-x_{in}\right)\delta\left(y-y_{in}\right) - \delta\left(x-x_{out}\right)\delta\left(y-y_{out}\right)\right)\cos\frac{k'\pi}{a}x\;\cos\frac{l'\pi}{b}y \\ &= \frac{\rho I c_{k'l'}}{ab}\int_0^a \delta\left(x-x_{in}\right)\cos\frac{k'\pi}{a}x\,dx\int_0^b \delta\left(y-y_{in}\right)\cos\frac{l'\pi}{b}y\,dy \\ &\quad - \frac{\rho I c_{k'l'}}{ab}\int_0^a \delta\left(x-x_{out}\right)\cos\frac{k'\pi}{a}x\,dx\int_0^b \delta\left(y-y_{out}\right)\;\cos\frac{l'\pi}{b}y\,dy \\ &= \frac{\rho I c_{k'l'}}{ab}\left(\cos\frac{k'\pi}{a}x_{in}\;\cos\frac{l'\pi}{b}y_{in} - \cos\frac{k'\pi}{a}x_{out}\;\cos\frac{l'\pi}{b}y_{out}\right)\end{aligned}$$

which simplifies the above with

$$q_{kl} = \frac{\rho I}{ab}\left(\cos\frac{k\pi}{a}x_{in}\;\cos\frac{l\pi}{b}y_{in} - \cos\frac{k\pi}{a}x_{out}\;\cos\frac{l\pi}{b}y_{out}\right)$$

to

$$\psi_{kl} = \begin{cases} 4q_{kl} & \text{for } k>0 \text{ and } l>0 \\ 2q_{kl} & \text{for } \{k=0 \text{ and } l>0\} \text{ or } \{k>0 \text{ and } l=0\} \\ q_{00} & \text{for } k'=0 \text{ and } l'=0 \end{cases}$$

In conclusion, we find the potential in (6)

$$V(x,y,z)=\sum_{k=0}^{\infty}\sum_{l=0}^{\infty}\varphi_{kl}\cos\frac{k\pi}{a}x\cos\frac{l\pi}{b}y\cosh\left(\sqrt{\left(\frac{k\pi}{a}\right)^2+\left(\frac{l\pi}{b}\right)^2}(z-c)\right)$$

with the coefficients

$$\varphi_{kl}=\begin{cases}4p_{kl} & \text{for } k>0 \text{ and } l>0\\ 2p_{kl} & \text{for } \{k=0 \text{ and } l>0\} \text{ or } \{k>0 \text{ and } l=0\}\\ p_{00} & \text{for } k'=0 \text{ and } l'=0\end{cases}$$

where, for $(k,l)\neq(0,0)$,

$$p_{kl}=\frac{\frac{\varrho I}{ab}\left(\cos\frac{k\pi}{a}x_{in}\ \cos\frac{l\pi}{b}y_{in}-\cos\frac{k\pi}{a}x_{out}\ \cos\frac{l\pi}{b}y_{out}\right)}{\sinh\left(c\sqrt{\left(\frac{k\pi}{a}\right)^2+\left(\frac{l\pi}{b}\right)^2}\right)\sqrt{\left(\frac{k\pi}{a}\right)^2+\left(\frac{l\pi}{b}\right)^2}}$$

Hence,

$$p_{k0}=\frac{\frac{\varrho I}{ab}\left(\cos\frac{k\pi}{a}x_{in}\ -\cos\frac{k\pi}{a}x_{out}\ \right)}{\frac{k\pi}{a}\sinh\left(c\frac{k\pi}{a}\right)}$$

and

$$p_{0l}=\frac{\frac{\varrho I}{ab}\left(\cos\frac{l\pi}{b}y_{in}-\cos\frac{l\pi}{b}y_{out}\right)}{\frac{l\pi}{b}\sinh\left(c\frac{l\pi}{b}\right)}$$

but p_{00} is constant, which will produce the reference potential V_{ref}.

3.5 Summary of the analytic solution in 3D

3.5.1 Potential $V(x,y,z)$ in 3D

The explicit solution of the potential at the point (x,y,z) inside and on the boundary of the beam, i.e. for $0\leq x\leq a$, $0\leq y\leq b$ and $0\leq z\leq c$, then is

$$\begin{aligned}V(x,y,z)+V_{\text{ref}}=&\frac{2\varrho I}{ab}\sum_{k=1}^{\infty}\frac{\left(\cos\frac{k\pi}{a}x_{in}\ -\cos\frac{k\pi}{a}x_{out}\ \right)}{\frac{k\pi}{a}\sinh\left(c\frac{k\pi}{a}\right)}\cos\frac{k\pi}{a}x\cosh\left(\frac{k\pi}{a}(z-c)\right)\\&+\frac{2\varrho I}{ab}\sum_{l=1}^{\infty}\frac{\left(\cos\frac{l\pi}{b}y_{in}-\cos\frac{l\pi}{b}y_{out}\right)}{\frac{l\pi}{b}\sinh\left(c\frac{l\pi}{b}\right)}\cos\frac{l\pi}{b}y\cosh\left(\frac{l\pi}{b}(z-c)\right)\\&+\frac{4\varrho I}{ab}\sum_{k=1}^{\infty}\sum_{l=1}^{\infty}\frac{\left(\cos\frac{k\pi}{a}x_{in}\ \cos\frac{l\pi}{b}y_{in}-\cos\frac{k\pi}{a}x_{out}\ \cos\frac{l\pi}{b}y_{out}\right)}{\sinh\left(c\sqrt{\left(\frac{k\pi}{a}\right)^2+\left(\frac{l\pi}{b}\right)^2}\right)\sqrt{\left(\frac{k\pi}{a}\right)^2+\left(\frac{l\pi}{b}\right)^2}}\\&\times\cos\frac{k\pi}{a}x\cos\frac{l\pi}{b}y\cosh\left(\sqrt{\left(\frac{k\pi}{a}\right)^2+\left(\frac{l\pi}{b}\right)^2}(z-c)\right)\end{aligned}\tag{10}$$

Perhaps needless to recall, the voltage is only defined with respect to some reference potential V_{ref}. The periodicity of the double Fourier series (10) for $V(x,y,z)$ in the beam implies that the extension of the real number x, y and z to all real numbers, beyond $0\leq x\leq a$, $0\leq y\leq b$ and $0\leq z\leq c$, leads to a coverage of the 3D space by a repeated parallellepipidum, which can be regarded as the 3D extension of elliptic functions in the complex plane (see Appendix C). In general, for sufficiently large difference $|z-c|$, the double Fourier series (10) in 3D converges reasonably well.

3.5.2 Current density in 3D

The current density, for $0 \leq x \leq a$, $0 \leq y \leq b$ and $0 \leq z \leq c$,

$$\overrightarrow{j}\,(x,y,z) = \sigma \operatorname{grad} V = -\sigma\left(\frac{\partial V}{\partial x}, \frac{\partial V}{\partial y}, \frac{\partial V}{\partial z}\right)$$

is a vector with magnitude equal to

$$\left|\overrightarrow{j}\,(x,y,z)\right| = |j\,(x,y,z)| = \sigma\sqrt{\left(\frac{\partial V}{\partial x}\right)^2 + \left(\frac{\partial V}{\partial y}\right)^2 + \left(\frac{\partial V}{\partial z}\right)^2}$$

The partial derivatives $\frac{\partial V}{\partial x}$, $\frac{\partial V}{\partial y}$ and $\frac{\partial V}{\partial z}$ are readily computed from (10), e.g.:

$$\begin{aligned}\frac{\partial V}{\partial x} = &-\frac{2\varrho I}{ab}\sum_{k=1}^{\infty}\frac{\left(\cos\frac{k\pi}{a}x_{in} - \cos\frac{k\pi}{a}x_{out}\right)}{\sinh\left(c\frac{k\pi}{a}\right)}\sin\frac{k\pi}{a}x\cosh\left(\frac{k\pi}{a}(z-c)\right)\\ &-\frac{4\varrho I}{ab}\sum_{k=1}^{\infty}\sum_{l=1}^{\infty}\frac{k\pi}{a}\frac{\left(\cos\frac{k\pi}{a}x_{in}\ \cos\frac{l\pi}{b}y_{in} - \cos\frac{k\pi}{a}x_{out}\ \cos\frac{l\pi}{b}y_{out}\right)}{\sinh\left(c\sqrt{\left(\frac{k\pi}{a}\right)^2 + \left(\frac{l\pi}{b}\right)^2}\right)\sqrt{\left(\frac{k\pi}{a}\right)^2 + \left(\frac{l\pi}{b}\right)^2}}\\ &\times\sin\frac{k\pi}{a}x\cos\frac{l\pi}{b}y\cosh\left(\sqrt{\left(\frac{k\pi}{a}\right)^2 + \left(\frac{l\pi}{b}\right)^2}(z-c)\right)\end{aligned}$$

Unfortunately, the series of $|j\,(x,y,z)|$ for $z = 0$ converge *too slowly to be of practical use*!

4 Reduction to two dimensions

The Laplace equation (1) in 2D, $\frac{\partial^2 V}{\partial x^2} + \frac{\partial^2 V}{\partial y^2} = 0$, has as general solution a harmonic function $V\,(x,y)$. A non-constant harmonic function $V\,(x,y)$ cannot have an extremum, either minimum or maximum, at an interior point of the region [7, p. 167]. Imposing that no current can enter the rectangle, i.e. $\frac{\partial V}{\partial x}\big|_{x=0} = \frac{\partial V}{\partial x}\big|_{x=a} = 0$ and $\frac{\partial V}{\partial y}\Big|_{y=0} = \frac{\partial V}{\partial y}\Big|_{y=b} = 0$, implies that the extreme value of the harmonic function $V\,(x,y)$ occurs at the boundary. Hence, current can only flow from one boundary to another, without an internal high potential at $s = (x_{in}, y_{in})$ and internal low potential at $d = (x_{out}, y_{out})$. Apart from the physical vector decomposition argument in the introduction, the harmonic function argument shows why a 3D computation is necessary for the current in- and ejection.

However, the current injection without vector decomposition into the plane can be regarded as a pile-up of charges at point s when the parallellepipidum is shrinked to a 2D rectangle. Hence, in 2D, we may consider a plate or rectangle with two opposite electric charges at s and d. The Laplacian equation is then replaced by a (normalized[5]) Poisson's equation $\Delta V = -\varphi\,(r)$, where the charge density $\varphi\,(r)$ in 2D consists of two point charges,

$$\Delta V = \frac{\partial^2 V}{\partial x^2} + \frac{\partial^2 V}{\partial y^2} = \delta\,(x_{in}, y_{in}) - \delta\,(x_{out}, y_{out})$$

with boundary conditions $\frac{\partial V}{\partial x}\big|_{x=0} = \frac{\partial V}{\partial x}\big|_{x=a} = 0$ and $\frac{\partial V}{\partial y}\Big|_{y=0} = \frac{\partial V}{\partial y}\Big|_{y=b} = 0$, indicating that no current can flow through the boundary. Our new formulation is related to the "Green's function for

[5] The permittivity ϵ_0 in $\Delta V = -\frac{1}{\epsilon_0}\rho$ has disappeared.

the Laplacian ΔV in the interior of a rectangle" briefly reviewed in Appendix B, whose solution [8, p. 384] involves elliptic functions when the boundary conditions are $V(0,y) = V(a,y) = V(x,0) = V(x,b) = 0$, i.e. $V = 0$ at the boundary of the rectangle. The double Fourier series of the Green function for our Neumann boundary conditions is computed in [9, p. 399]. We first derive that double Fourier series.

4.1 Potential $V(x,y)$ in 2D

The voltage in the xy-plane (i.e. $z = 0$) follows from the 3D voltage (10), for $0 \leq x \leq a$ and $0 \leq y \leq b$, as

$$\begin{aligned} V(x,y,0) + V_{\text{ref}} = & \frac{2\varrho I}{ab} \sum_{k=1}^{\infty} \frac{\left(\cos\frac{k\pi}{a}x_{in} - \cos\frac{k\pi}{a}x_{out}\right)}{\frac{k\pi}{a}\tanh\left(c\frac{k\pi}{a}\right)} \cos\frac{k\pi}{a}x \\ & + \frac{2\varrho I}{ab} \sum_{l=1}^{\infty} \frac{\left(\cos\frac{l\pi}{b}y_{in} - \cos\frac{l\pi}{b}y_{out}\right)}{\frac{l\pi}{b}\tanh\left(c\frac{l\pi}{b}\right)} \cos\frac{l\pi}{b}y \\ & + \frac{4\varrho I}{ab} \sum_{k=1}^{\infty}\sum_{l=1}^{\infty} \frac{\left(\cos\frac{k\pi}{a}x_{in}\ \cos\frac{l\pi}{b}y_{in} - \cos\frac{k\pi}{a}x_{out}\ \cos\frac{l\pi}{b}y_{out}\right)}{\tanh\left(c\sqrt{\left(\frac{k\pi}{a}\right)^2 + \left(\frac{l\pi}{b}\right)^2}\right)\sqrt{\left(\frac{k\pi}{a}\right)^2 + \left(\frac{l\pi}{b}\right)^2}} \cos\frac{k\pi}{a}x\cos\frac{l\pi}{b}y \end{aligned}$$

The Taylor series $\pi\cot(\pi x) = \frac{1}{x} - 2\sum_{n=1}^{\infty}\zeta(2n)\,x^{2n-1}$, valid[6] for $|x| < 1$ and where $\zeta(s)$ is the Riemann Zeta-function [11], indicates, with $\pi\cot(i\pi x) = \frac{\pi}{i}\coth(\pi x)$, that

$$\coth(z) = \frac{1}{\tanh(z)} = \frac{1}{z} - 2\sum_{n=1}^{\infty}\frac{\zeta(2n)}{\pi^{2n}}(-1)^n\, z^{2n-1} \text{ for } |z| < \pi$$

Hence, for small c, we find that

$$\begin{aligned} V(x,y,0) + V_{\text{ref}} = & \frac{2\varrho I}{abc} \sum_{k=1}^{\infty} \frac{\left(\cos\frac{k\pi}{a}x_{in} - \cos\frac{k\pi}{a}x_{out}\right)}{\left(\frac{k\pi}{a}\right)^2} \cos\frac{k\pi}{a}x + O(c) \\ & + \frac{2\varrho I}{abc} \sum_{l=1}^{\infty} \frac{\left(\cos\frac{l\pi}{b}y_{in} - \cos\frac{l\pi}{b}y_{out}\right)}{\left(\frac{l\pi}{b}\right)^2} \cos\frac{l\pi}{b}y \\ & + \frac{4\varrho I}{abc} \sum_{k=1}^{\infty}\sum_{l=1}^{\infty} \frac{\left(\cos\frac{k\pi}{a}x_{in}\ \cos\frac{l\pi}{b}y_{in} - \cos\frac{k\pi}{a}x_{out}\ \cos\frac{l\pi}{b}y_{out}\right)}{\left(\frac{k\pi}{a}\right)^2 + \left(\frac{l\pi}{b}\right)^2} \cos\frac{k\pi}{a}x\cos\frac{l\pi}{b}y \end{aligned} \quad (11)$$

where the volume of the parallelepiped is $v_{3D} = abc$. For $c \to 0$, i.e. omitting the order terms $O(c)$ in (11), and after renormalization by $\frac{\varrho I}{c} = 1$, we denote the 2D voltage as $V(x,y) = \lim_{c\to 0} V(x,y,0)$, subject to $\frac{\varrho I}{c} = 1$, whose result is

$$\begin{aligned} V(x,y) + V_{\text{ref}} = & \frac{2}{ab}\left(\sum_{k=1}^{\infty} \frac{\left(\cos\frac{k\pi}{a}x_{in} - \cos\frac{k\pi}{a}x_{out}\right)}{\left(\frac{k\pi}{a}\right)^2} \cos\frac{k\pi}{a}x + \sum_{l=1}^{\infty} \frac{\left(\cos\frac{l\pi}{b}y_{in} - \cos\frac{l\pi}{b}y_{out}\right)}{\left(\frac{l\pi}{b}\right)^2} \cos\frac{l\pi}{b}y\right) \\ & + \frac{4}{ab} \sum_{k=1}^{\infty}\sum_{l=1}^{\infty} \frac{\left(\cos\frac{k\pi}{a}x_{in}\ \cos\frac{l\pi}{b}y_{in} - \cos\frac{k\pi}{a}x_{out}\ \cos\frac{l\pi}{b}y_{out}\right)}{\left(\frac{k\pi}{a}\right)^2 + \left(\frac{l\pi}{b}\right)^2} \cos\frac{k\pi}{a}x\cos\frac{l\pi}{b}y \end{aligned} \quad (12)$$

which is precisely

$$V(x,y) = K(x,y;x_{in},y_{in}) - K(x,y;x_{out},y_{out}) \quad (13)$$

[6] The Taylor series follows directly from the generating function (54) below of the Bernoulli numbers [10, art. 240].

in the Green's function approach (30). In summary, we have shown mathematically that the dimension reduction from 3D to 2D indeed is equivalent to placing point charges at s and d.

We explain the renormalization of $\frac{\varrho I}{c} = 1$. In order that $\lim_{c\to 0} \frac{\varrho I}{c}$ is finite, the current I must tend to zero, given that the resistivity ϱ of the material is fixed[7], also in 2D. In other words, there is no injected current anymore, but only not-moving charges. In any case, a current injected orthogonal to the plane must bend in a single point over 90 degrees which is mechanically speaking or in vector terminology not possible: hence, the current accumulates to a charge peak at that single point s.

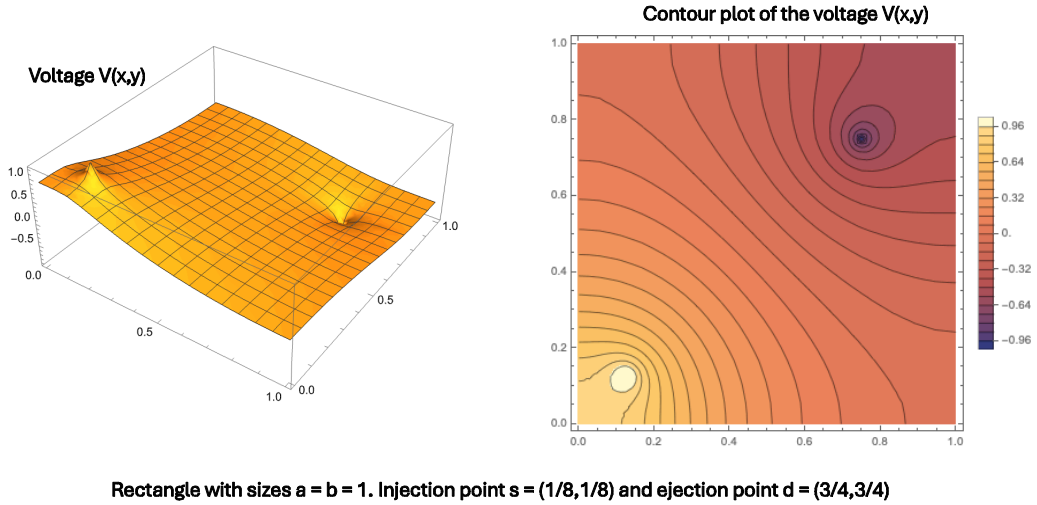


Figure 2: Example of the voltage $V(x, y)$, computed from (12) with $K = 100$ terms in the Fourier series.

Although our voltage (10) in 3D and the 2D reduction (12) are exact, the double Fourier series converge very slowly for $V(x, y, 0)$, i.e. in the xy-plane. Fig. 2 shows both a 3D plot and the contour plot of the potential $V(x, y) = V(x, y, 0)$ in (12) for $c \to 0$ or in (13) in a square with sizes $a = b = 1$. The current injection is in $s = (x_{in}, y_{in}) = (1/8, 1/8)$ and current ejection occurs at $d = (x_{out}, y_{out}) = (3/4, 3/4)$. We underline that the computation of the voltage $V(x, y)$ is involved, but possible in a reasonable time, whereas the current density is problematic, due to the *extremely slow convergence*. Fortunately, Fig. 3 computed with the single Fourier series (26) below draws the current density corresponding to the voltage in Fig. 2.

We remark that Mathematica in Fig. 3 plots white lines at the peculiar discontinuities of the Fourier coefficients, the functions g_n in (21) and h_n in (23), whereas those discontinuities disappear in the Fourier series (with infinite terms), because both the voltage $V(x, y)$ and the magnitude $|j(x, y)|$ of the current density are continuous[8] for any x and y in the rectangle, apart from the in- and ejection points s and d. The inaccuracies at the white lines in Fig. 3 has motivated further analysis, that eventually led to a much faster converging, so called q-series in Appendix D. Fig. 4 illustrates the smoothness around the white lines, computed with the q-series method.

[7] A zero resistivity $\varrho = 0$ would imply superconductivity, which we exclude.

[8] Indeed, the potential $V(x, y)$ satisfies the Poisson second-order differential equation and any differentiable function (such as the partial derivatives $\frac{\partial V}{\partial x}$ and $\frac{\partial V}{\partial y}$) is continuous.

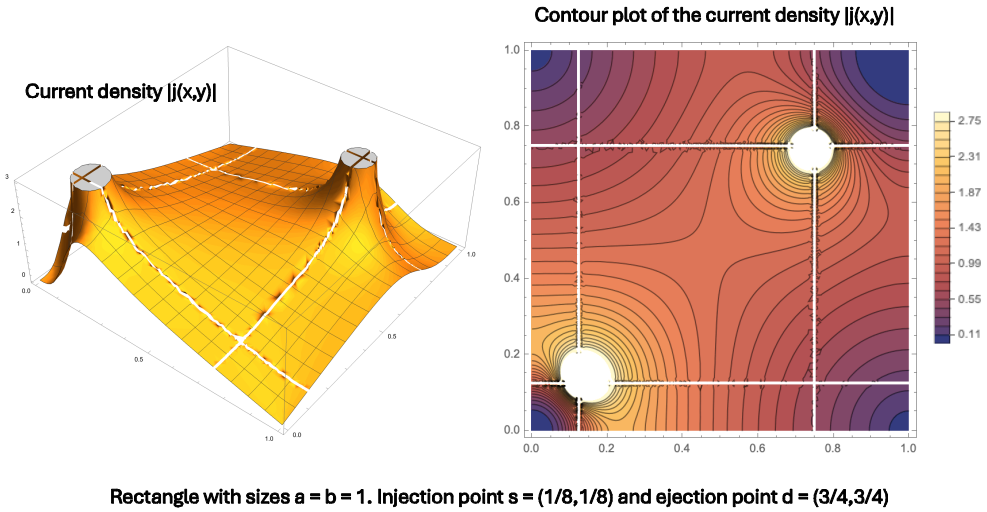


Figure 3: The magnitude $|j(x,y)|$ of the current density corresponding to Fig. 2, computed from (26) with $K = 100$ terms.

4.2 From a double to single Fourier series with quasi-Green's function

The very slow convergence of partial derivatives of the double Fourier series (12)-(13) has motivated the search for a faster computation, without loosing accuracy. Following Morse and Feshbach [12, p. 799-800] and recalling the rewriting (31) of the 2D voltage (12) with coefficients γ_{nm},

$$K(x,y;\xi,\eta) = \sum_{n=0}^{\infty}\left(\frac{4}{ab}\sum_{m=0}^{\infty}\gamma_{nm}\frac{\cos\left(\frac{\pi n}{a}\xi\right)\cos\left(\frac{\pi m}{b}y\right)\cos\left(\frac{\pi m}{b}\eta\right)}{\left(\frac{\pi n}{a}\right)^2+\left(\frac{\pi m}{b}\right)^2}\right)\cos\left(\frac{\pi n}{a}x\right)$$

we propose the solution

$$F(x,y) = \sum_{n=0}^{\infty} f_n(y)\cos\left(\frac{\pi n}{a}x\right)$$

of the Poisson equation with general charge density $\varphi(x,y)$,

$$\frac{\partial^2 F}{\partial x^2}+\frac{\partial^2 F}{\partial y^2} = -\varphi(x,y) \tag{14}$$

The Neumann boundary conditions $\operatorname{grad} F = 0$ at the boundary of the rectangle $(0,0),(0,b),(a,b)$ and $(a,0)$ reflect that no current can flow through the boundaries of the rectangle. In addition, we propose

$$\varphi(x,y) = \sum_{n=0}^{\infty}\rho_n(y)\cos\left(\frac{\pi n}{a}x\right) \tag{15}$$

where it holds, via orthogonality of Fourier series in Section A.1,

$$\begin{aligned}\int_0^a \varphi(x,y)\cos\left(\frac{\pi k}{a}x\right)dx &= \sum_{n=0}^{\infty}\rho_n(y)\int_0^a \cos\left(\frac{\pi k}{a}x\right)\cos\left(\frac{\pi n}{a}x\right)dx \\ &= \frac{1}{2}\sum_{n=0}^{\infty}\rho_n(y)\int_0^a \cos\left(\frac{\pi(k-n)}{a}x\right)dx + \frac{1}{2}\sum_{n=0}^{\infty}\rho_n(y)\int_0^a \cos\left(\frac{\pi(k+n)}{a}x\right)dx \\ &= \frac{1}{2}\sum_{n=0}^{\infty}\rho_n(y)\frac{\sin(\pi(k-n))}{\frac{\pi(k-n)}{a}} + \frac{1}{2}\sum_{n=0}^{\infty}\rho_n(y)\frac{\sin(\pi(k+n))}{\frac{\pi(k+n)}{a}} = \frac{a}{2}\rho_k(y)\end{aligned}$$

Thus, for $k \geq 1$, we obtain that

$$\rho_k(y) = \frac{2}{a}\int_0^a \varphi(x,y)\cos\left(\frac{\pi k}{a}x\right)dx$$

and, for $k = 0$,

$$\rho_0(y) = \frac{1}{a}\int_0^a \varphi(x,y)\,dx$$

However, our Neumann boundaries (i.e. grad $F = 0$; no current through the boundary) are different from the theory in Morse and Feshbach [12, p. 799-800], which is based on Dirichlet boundaries (i.e. $F = 0$; the voltage is zero at the boundary), exemplified in Appendix B. That difference causes a major complication, because there does not exist a Green's function in our setting as shown below, but we can define a "quasi" Green's function with two opposite delta functions instead of a single one in the classical definition (28) of a Green's function. Since the current density is our main target, which is a partial derivative of the potential, the unknown appearing constant below and the non-existence of a Green's function, is alleviated. After removing this barrier, we may continue with our "quasi" Green's functions.

Introducing the proposal (15) into the Poisson differential equation (14)

$$-\sum_{n=0}^{\infty} f_n(y)\left(\frac{\pi n}{a}\right)^2\cos\left(\frac{\pi n}{a}x\right) + \sum_{n=0}^{\infty}\frac{d^2 f_n(y)}{dy^2}\cos\left(\frac{\pi n}{a}x\right) = -\sum_{n=0}^{\infty}\rho_n(y)\cos\left(\frac{\pi n}{a}x\right)$$

leads to the second-order differential equation

$$\frac{d^2 f_n(y)}{dy^2} - \left(\frac{\pi n}{a}\right)^2 f_n(y) = -\rho_n(y) \tag{16}$$

The boundary conditions $\frac{\partial F}{\partial y} = -\sum_{n=0}^{\infty}\frac{df_n(y)}{dy}\cos\left(\frac{\pi n}{a}x\right) = 0$ for $y = 0$ and $y = b$ and all $x \in [0,a]$ translate to $\frac{df_n(y)}{dy} = 0$ for $y = 0$ and $y = b$ for all integer $n \geq 0$. The homogeneous solution, satisfying $\frac{d^2 h_n(y)}{dy^2} - \left(\frac{\pi n}{a}\right)^2 h_n(y) = 0$ is

$$h_n(y) = A\cosh\frac{\pi n}{a}y + B\cosh\frac{\pi n}{a}(b-y)$$

where $y_1 = \cosh\frac{\pi n}{a}y$ and $y_2 = \cosh\frac{\pi n}{a}(b-y)$ are independent solutions with Wronskian $W(y_1,y_2) = \begin{vmatrix} y_1 & y_2 \\ y_1' & y_2' \end{vmatrix} = y_1 y_2' - y_2 y_1'$ equal to

$$\begin{aligned}W(y_1,y_2) &= -\frac{\pi n}{a}\left(\cosh\frac{\pi n}{a}y\sinh\frac{\pi n}{a}(b-y) + \cosh\frac{\pi n}{a}(b-y)\sinh\frac{\pi n}{a}y\right) \\ &= -\frac{\pi n}{a}\sinh\left(\frac{\pi n}{a}(b-y) + \frac{\pi n}{a}y\right) = -\frac{\pi n}{a}\sinh\left(\frac{\pi n}{a}b\right)\end{aligned}$$

and constant (as it must be [12]). Only for $n = 0$, both $y_1 = y_2$ are dependent! However, for $n = 0$, the second-order differential equation (16) simplifies to

$$\frac{d^2 f_0(y)}{dy^2} = -\rho_0(y) = -\frac{1}{a}\int_0^a \varphi(x,y)\,dx$$

and integration yields

$$\frac{df_0(y)}{dy} - \left.\frac{df_0(y)}{dy}\right|_{y=0} = -\frac{1}{a}\int_0^a\int_0^y \varphi(x,u)\,dxdu$$

The boundary condition $\frac{df_0(y)}{dy} = 0$ for $y = 0$ leads to

$$\frac{df_0(y)}{dy} = -\frac{1}{a}\int_0^a\int_0^y \varphi(x,u)\,dxdu \tag{17}$$

However, the boundary condition $\frac{df_0(y)}{dy} = 0$ at $y = b$ requires that $\int_0^a\int_0^b \varphi(x,y)\,dxdy = 0$, which is physically correct, if the sum of all charges in the beam is zero. This implies that a single delta function as for the Green's function in (28) is incompatible. Since our solution will always requires an injection and ejection, implying a difference between two delta charges, we ignore this incompatibility and the requirement $\int_0^a\int_0^b \varphi(x,y)\,dxdy = 0$ for the moment. After an additional integration of the both sides of (17), we find

$$f_0(y) - f_0(0) = -\frac{1}{a}\int_0^a\int_0^y dt\int_0^t \varphi(x,u)\,dxdu$$

Partial integration yields

$$\begin{aligned} f_0(y) - f_0(0) &= -\frac{1}{a}\int_0^a \left(t\int_0^t \varphi(x,u)\,du\Big|_0^y - \int_0^y t\varphi(x,t)\,dt\right)dx \\ &= -\frac{1}{a}\int_0^a dx\int_0^y dt\,(y-t)\,\varphi(x,t) \end{aligned}$$

In summary, we arrive for $n = 0$, where the constant $f_0(0) = c$ arises due to the omission of the boundary condition $\left.\frac{df_0(y)}{dy}\right|_{y=b} = 0$, at

$$f_0(y) = c - \frac{1}{a}\int_0^a dx\int_0^y dt\,(y-t)\,\varphi(x,t) \tag{18}$$

We substitute the functions $y_1 = \cosh\frac{\pi n}{a}y$ and $y_2 = \cosh\frac{\pi n}{a}(b-y)$ in the general solution [12, eq. (5.2.19)]

$$\psi(t) = y_1\left(c_1 - \int\frac{ry_2}{W(y_1,y_2)}dt\right) + y_2\left(c_2 + \int\frac{ry_1}{W(y_1,y_2)}dt\right)$$

of a second order differential equation $\frac{d^2\psi}{dt^2} + p(t)\frac{d\psi}{dt} + q(t)\psi(t) = r(t)$, where the indefinite integrals and constants c_1 and c_2 may be adjusted to fit the boundary conditions. Applying the general theory, with integration limits that obey the boundary conditions, we obtain

$$\begin{aligned} f_n(y) = \cosh\frac{\pi n}{a}y &\left(c_1 + \frac{1}{\frac{\pi n}{a}\sinh\left(\frac{\pi n}{a}b\right)}\int_y^b \rho_n(t)\cosh\frac{\pi n}{a}(b-t)\,dt\right) \\ &+ \cosh\frac{\pi n}{a}(b-y)\left(c_2 + \frac{1}{\frac{\pi n}{a}\sinh\left(\frac{\pi n}{a}b\right)}\int_0^y \rho_n(t)\cosh\frac{\pi n}{a}tdt\right) \end{aligned}$$

The boundary condition $f_n'(0) = f_n'(b) = 0$ requires the computation of the derivative[9],

$$f_n'(y) = \frac{\pi n}{a}\sinh\frac{\pi n}{a}y\left(c_1 + \frac{1}{\frac{\pi n}{a}\sinh\left(\frac{\pi n}{a}b\right)}\int_y^b \rho_n(t)\cosh\frac{\pi n}{a}(b-t)\,dt\right)$$
$$-\frac{\pi n}{a}\sinh\frac{\pi n}{a}(b-y)\left(c_2 + \frac{1}{\frac{\pi n}{a}\sinh\left(\frac{\pi n}{a}b\right)}\int_0^y \rho_n(t)\cosh\frac{\pi n}{a}tdt\right)$$

The first boundary condition $f_n'(0) = -\frac{\pi n}{a}\sinh\frac{\pi n}{a}b\ \ (c_2) = 0$ requires that $c_2 = 0$. Similarly, the second, boundary condition $f_n'(b) = \frac{\pi n}{a}\sinh\frac{\pi n}{a}b\ \ (c_1) = 0$ requires that $c_1 = 0$. Thus, with $c_1 = c_2 = 0$, we obtain the solution, for $n > 0$,

$$f_n(y) = \frac{\int_0^y \rho_n(t)\cosh\frac{\pi n}{a}(b-y)\cosh\frac{\pi n}{a}tdt + \int_y^b \rho_n(t)\cosh\frac{\pi n}{a}y\cosh\frac{\pi n}{a}(b-t)\,dt}{\frac{\pi n}{a}\sinh\left(\frac{\pi n}{a}b\right)} \tag{19}$$

which we write as

$$f_n(y) = \int_0^b g_n(y,t)\,\rho_n(t)$$

where

$$g_n(y,t) = \frac{1}{\frac{\pi n}{a}\sinh\left(\frac{\pi n}{a}b\right)}\begin{cases}\cosh\frac{\pi n}{a}(b-y)\cosh\frac{\pi n}{a}t & \text{for } 0 \le t \le y\\ \cosh\frac{\pi n}{a}y\cosh\frac{\pi n}{a}(b-t) & \text{for } y < t \le b\end{cases}$$

One may verify that $f_n(y)$ in (19) satisfies the differential equation $\frac{d^2 f_n(y)}{dy^2} - \left(\frac{\pi n}{a}\right)^2 f_n(y) = -\rho_n(y)$.

Introducing $\rho_n(y) = \frac{2}{a}\int_0^a \varphi(x,y)\cos\left(\frac{\pi n}{a}x\right)dx$ into $f_n(y) = \int_0^b g_n(y,t)\,\rho_n(t)\,dt$ yields, for $n > 0$,

$$f_n(y) = \frac{2}{a}\int_0^a d\xi\int_0^b d\eta\ \varphi(\xi,\eta)\,g_n(y,\eta)\cos\left(\frac{\pi n}{a}\xi\right)$$

The case $f_0(y) = c - \frac{1}{a}\int_0^a d\xi\int_0^y d\eta\varphi(\xi,\eta)(y-\eta)$ in (18) for $n = 0$ shows that

$$f_0(y) = c - \frac{1}{a}\int_0^a d\xi\int_0^b d\eta\varphi(\xi,\eta)(y-\eta)$$

which defines

$$g_0(y,\eta) = \begin{cases}\eta - y & \text{for } 0 \le \eta \le y\\ 0 & \text{for } y < \eta \le b\end{cases}$$

---

[9] Indeed,

$$f_n'(y) = \frac{\pi n}{a}\sinh\frac{\pi n}{a}y\left(c_1 + \frac{1}{\frac{\pi n}{a}\sinh\left(\frac{\pi n}{a}b\right)}\int_y^b \rho_n(t)\cosh\frac{\pi n}{a}(b-t)\,dt\right)$$
$$-\cosh\frac{\pi n}{a}y\left(\frac{1}{\frac{\pi n}{a}\sinh\left(\frac{\pi n}{a}b\right)}\rho_n(y)\cosh\frac{\pi n}{a}(b-y)\right)$$
$$-\frac{\pi n}{a}\sinh\frac{\pi n}{a}(b-y)\left(c_2 + \frac{1}{\frac{\pi n}{a}\sinh\left(\frac{\pi n}{a}b\right)}\int_0^y \rho_n(t)\cosh\frac{\pi n}{a}tdt\right)$$
$$+\cosh\frac{\pi n}{a}(b-y)\left(\frac{1}{\frac{\pi n}{a}\sinh\left(\frac{\pi n}{a}b\right)}\rho_n(y)\cosh\frac{\pi n}{a}y\right)$$

After cancellation of the second and fourth term, we find the derivative.

Combining all pieces into the proposal leads to

$$F(x,y) = f_0(y) + \sum_{n=1}^{\infty} f_n(y) \cos\left(\frac{\pi n}{a}x\right)$$
$$= c + \int_0^a d\xi \int_0^b d\eta \varphi(\xi,\eta) \frac{1}{a} g_0(y,\eta) + \int_0^a d\xi \int_0^b d\eta\, \varphi(\xi,\eta) \frac{2}{a} \sum_{n=1}^{\infty} g_n(y,\eta) \cos\left(\frac{\pi n}{a}\xi\right) \cos\left(\frac{\pi n}{a}x\right)$$

Green's function theory tells us that the general solution (29) can be written as

$$F(x,y) = \int_0^a d\xi \int_0^b d\eta\, \varphi(\xi,\eta) K(x,y,\xi,\eta)$$

Although a Green's function obeying a Poisson equation (28) with a single delta function does not exist for our boundary problem and at least two opposite delta functions are needed to satisfy the $n = 0$ boundary condition, reflecting that the total amount of charges in the rectangle is zero, i.e. $\frac{df_0(y)}{dy}\Big|_{y=b} = \int_0^a d\xi \int_0^b d\eta \varphi(\xi,\eta) = 0$, we proceed with the suggestion that the constant $c = 0$ to arrive at the "quasi"-Green's function

$$K(x,y,\xi,\eta) = \frac{1}{a} g_0(y,\eta) + \frac{2}{a} \sum_{n=1}^{\infty} g_n(y,\eta) \cos\left(\frac{\pi n}{a}\xi\right) \cos\left(\frac{\pi n}{a}x\right) \tag{20}$$

where

$$g_n(y,\eta) = \frac{1}{\frac{\pi n}{a} \sinh\left(\frac{\pi n}{a} b\right)} \begin{cases} \cosh\frac{\pi n}{a}(b-y) \cosh\frac{\pi n}{a}\eta & \text{for } 0 \le \eta \le y \\ \cosh\frac{\pi n}{a}(b-\eta) \cosh\frac{\pi n}{a} y & \text{for } y < \eta \le b \end{cases} \tag{21}$$

The "quasi"-Green's function thus obeys the Poisson equation

$$\Delta K(r; r_s, r_d) = -\left(\delta(r - r_s) - \delta(r - r_d)\right)$$

with a delta function at the source node s and an opposite delta function at the drain node d. The reversal of y and η in (21) shows that $g_n(y,\eta)$ for $n > 0$ in the regime $0 \le \eta \le y$ equals $g_n(\eta, y)$ in the interval $y < \eta \le b$.

Finally, due to symmetry, replacing x by y, ξ by η and a by b (and vice versa) results into the dual single quasi-Green's function

$$K(x,y,\xi,\eta) = \frac{1}{b} g_0(x,\xi) + \frac{2}{b} \sum_{n=1}^{\infty} h_n(x,\xi) \cos\left(\frac{\pi n}{b}\eta\right) \cos\left(\frac{\pi n}{b} y\right) \tag{22}$$

where

$$h_n(x,\xi) = \frac{1}{\frac{\pi n}{b} \sinh\left(\frac{\pi n}{b} a\right)} \begin{cases} \cosh\frac{\pi n}{b}(a-x) \cosh\frac{\pi n}{b}\xi & \text{for } 0 \le \xi \le x \\ \cosh\frac{\pi n}{b} x \cosh\frac{\pi n}{b}(a-\xi) & \text{for } x < \xi \le a \end{cases} \tag{23}$$

The correctness of (22) may be verified by starting from the proposal $F(x,y) = \sum_{n=0}^{\infty} r_n(x) \cos\left(\frac{\pi n}{b} y\right)$ in the Poisson equation (14) and mimicking the steps followed that led to the "quasi"-Green's function (20).

Numerical computations indicate that the voltage (13), computed by the single sum Green's function (20), only differs from the voltage (12), which equals the voltage (13) computed by the double sum Green's function (30), by a constant that only depends upon the injection and ejection points (s,d). Thus, for a given pair of injection points (s,d) the voltage is only defined with respect to a reference potential. In conclusion, we may proceed with the much faster converging single Green's function (20).

4.3 Convergence of the quasi-Green's function (20) and (22)

The Fourier coefficients $g_n(y,\eta)$ in the quasi-Green's function (20) are peculiar around the point $y=\eta$, which corresponds to the y-coordinate of a point charge or delta function. The derivative

$$\frac{dg_n(y,\eta)}{dy} = \frac{1}{\sinh\left(\frac{\pi n}{a}b\right)} \begin{cases} -\sinh\frac{\pi n}{a}(b-y)\cosh\frac{\pi n}{a}\eta & \text{for } 0\le\eta\le y \\ \sinh\frac{\pi n}{a}y\cosh\frac{\pi n}{a}(b-\eta) & \text{for } y<\eta\le b \end{cases}$$

indicates that the left-derivative at $y=\eta$

$$\lim_{y\to\eta-\varepsilon}\frac{dg_n(y,\eta)}{dy} = -\frac{\sinh\frac{\pi n}{a}(b-\eta)\cosh\frac{\pi n}{a}\eta}{\sinh\left(\frac{\pi n}{a}b\right)}$$

and the right-derivative at $y=\eta$

$$\lim_{y\to\eta+\varepsilon}\frac{dg_n(y,\eta)}{dy} = \frac{\cosh\frac{\pi n}{a}(b-\eta)\sinh\frac{\pi n}{a}\eta}{\sinh\left(\frac{\pi n}{a}b\right)}$$

are different, implying that the function $g_n(y,\eta)$ is not differentiable at $y=\eta$. Although not differentiable, the function $g_n(y,\eta)$ in (21) remains continuous at $y=\eta$,

$$\lim_{y\to\eta}g_n(y,\eta) = g_n(\eta,\eta) = \frac{\cosh\frac{\pi n}{a}(b-\eta)\cosh\frac{\pi n}{a}\eta}{\frac{\pi n}{a}\sinh\left(\frac{\pi n}{a}b\right)}$$

Perhaps, the more important impact is the computation of the Fourier series at $y=\eta$. The function $g_n(y,\eta)$ in (21), rewritten as

$$g_n(y,\eta) = \frac{1}{\frac{\pi n}{a}\left(e^{\frac{\pi n}{a}b}-e^{-\frac{\pi n}{a}b}\right)} \begin{cases} \left(e^{\frac{\pi n}{a}(b-y)}+e^{-\frac{\pi n}{a}(b-y)}\right)\left(e^{\frac{\pi n}{a}\eta}+e^{-\frac{\pi n}{a}\eta}\right) & \text{for } 0\le\eta<y \\ \left(e^{\frac{\pi n}{a}(b-\eta)}+e^{-\frac{\pi n}{a}(b-\eta)}\right)\left(e^{\frac{\pi n}{a}y}+e^{-\frac{\pi n}{a}y}\right) & \text{for } y<\eta\le b \end{cases}$$

simplifies, for large n, to

$$g_n(y,\eta) \simeq \frac{1}{\frac{\pi n}{a}} \begin{pmatrix} e^{\frac{\pi n}{a}(\eta-y)} & \text{for } 0\le\eta<y \\ e^{\frac{\pi n}{a}(y-\eta)} & \text{for } y<\eta\le b \end{pmatrix} = \frac{a}{\pi n}e^{-\frac{\pi n}{a}|\eta-y|}$$

Hence, the Fourier series (20), for $0\le x\le a$ and $0\le y\le b$, is approximated by

$$K(x,y,\xi,\eta) \simeq \frac{1}{a}g_0(y,\eta)+\frac{2}{a}\sum_{n=1}^{n_o-1}g_n(y,\eta)\cos\left(\frac{\pi n}{a}\xi\right)\cos\left(\frac{\pi n}{a}x\right)+\frac{2}{\pi}\sum_{n=n_o}^{\infty}\frac{e^{-\frac{\pi n}{a}|\eta-y|}}{n}\cos\left(\frac{\pi n}{a}\xi\right)\cos\left(\frac{\pi n}{a}x\right)$$

The last sum

$$\left|\sum_{n=n_o}^{\infty}\frac{e^{-\frac{\pi n}{a}|\eta-y|}}{n}\cos\left(\frac{\pi n}{a}\xi\right)\cos\left(\frac{\pi n}{a}x\right)\right| \le \sum_{n=n_o}^{\infty}\frac{\left(e^{-\frac{\pi}{a}|\eta-y|}\right)^n}{n} < \sum_{n=1}^{\infty}\frac{\left(e^{-\frac{\pi}{a}|\eta-y|}\right)^n}{n}$$
$$= -\log\left(1-e^{-\frac{\pi}{a}|\eta-y|}\right)$$

indicates that, due to the decreasing exponential factor $e^{-\frac{\pi n}{a}|\eta-y|}$, the convergence is fast, provided that $|\eta-y|$ is sufficiently large. However, at $y=\eta$, the convergence of the Fourier series is very slow; the Fourier series even diverges for $x=\xi$ as shown below. The Fourier series (20) at $y=\eta$ becomes

$$K(x,\eta,\xi,\eta) \simeq \frac{2}{a}\sum_{n=1}^{n_o-1}g_n(\eta,\eta)\cos\left(\frac{\pi n}{a}\xi\right)\cos\left(\frac{\pi n}{a}x\right)+\frac{2}{\pi}\sum_{n=n_o}^{\infty}\frac{\cos\left(\frac{\pi n}{a}\xi\right)\cos\left(\frac{\pi n}{a}x\right)}{n}$$

After replacing $\cos\left(\frac{\pi n}{a}\xi\right)\cos\left(\frac{\pi n}{a}x\right) = \frac{1}{2}\cos\left(\frac{\pi n}{a}(\xi+x)\right) + \frac{1}{2}\cos\left(\frac{\pi n}{a}(\xi-x)\right)$, the last series can be approximated as

$$\sum_{n=n_o}^{\infty}\frac{\cos\left(\frac{\pi n}{a}\xi\right)\cos\left(\frac{\pi n}{a}x\right)}{n} = \frac{1}{2}\sum_{n=n_o}^{\infty}\frac{\cos\left(\frac{\pi n}{a}(\xi+x)\right)}{n} + \frac{1}{2}\sum_{n=n_o}^{\infty}\frac{\cos\left(\frac{\pi n}{a}(\xi-x)\right)}{n}$$
$$\approx -\frac{1}{2}\log\left(4\left|\sin\frac{\pi(\xi+x)}{2a}\right|\left|\sin\frac{\pi(\xi-x)}{2a}\right|\right)$$

where the last line has approximated $n_0 = 1$ and invoked (27) in Appendix A.2. The approximation clearly demonstrates that a point charge or delta function at $(x, y) = (\xi, \eta)$, then $K(\xi, \eta, \xi, \eta) \to \infty$.

In stead of approximating the sum as above, we compute the single Fourier series *exactly* in Appendix D. The surprise was the discovery of the q-series in (24) for the quasi-Green's function (20), that are intimately related to Gaussian polynomials and the Jacobi theta functions, which are the building system for elliptic functions as explained Appendix G. As deduced in Appendix D.1, the single sum quasi-Green's function (22) in the interval $0 \le \eta \le y$ can be written, with $q = e^{-2\frac{\pi b}{a}}$ as

$$K(x, y, \xi, \eta) = \frac{1}{a}g_0(y, \eta) + T_q(x, y; \xi, \eta) + T_q(x, y; \xi, -\eta) + T_q(-x, y; \xi, \eta) + T_q(-x, y; \xi, -\eta) \quad (24)$$

where the q-function $T_q(x, y; \xi, \eta)$ is

$$T_q(x, y; \xi, \eta) = -\frac{1}{4\pi}\log\left(1 - 2\cos\left(\frac{\pi}{a}(\xi+x)\right)e^{-\frac{\pi}{a}(y-\eta)} + e^{-2\frac{\pi}{a}(y-\eta)}\right) \quad (25)$$
$$-\frac{1}{4\pi}\log\prod_{k=1}^{\infty}\left(1 - 2\cos\left(\frac{\pi}{a}(\xi+x)\right)e^{\frac{\pi}{a}(y-\eta)}q^k + e^{2\frac{\pi}{a}(y-\eta)}q^{2k}\right)$$
$$\times\left(1 - 2\cos\left(\frac{\pi}{a}(\xi+x)\right)e^{-\frac{\pi}{a}(y-\eta)}q^k + e^{-2\frac{\pi}{a}(y-\eta)}q^{2k}\right)$$

Due to the fast converging sum (53) of the basic q-product in Section F and Section G, the infinite product in $T_q(x, y; \xi, \eta)$ converges very quickly and only a few factors in product (25) are needed.

4.4 Current density in 2D

We proceed to compute the current density in the rectangle, for $0 \le x \le a$ and $0 \le y \le b$,

$$\overrightarrow{j}(x, y) = \sigma \operatorname{grad} V = -\sigma\left(\frac{\partial V}{\partial x}, \frac{\partial V}{\partial y}\right)$$

which is a two dimensional vector with magnitude

$$\left|\overrightarrow{j}(x, y)\right| = |j(x, y)| = \sigma\sqrt{\left(\frac{\partial V}{\partial x}\right)^2 + \left(\frac{\partial V}{\partial y}\right)^2}$$

The partial derivative with respect to x of the single "quasi"- Green's function (20) is

$$\frac{\partial K(x, y, \xi, \eta)}{\partial x} = \frac{2\pi}{a^2}\sum_{n=1}^{\infty} n\, g_n(y, \eta)\cos\left(\frac{\pi n}{a}\xi\right)\sin\left(\frac{\pi n}{a}x\right)$$

However, $\frac{\partial K(x,y,\xi,\eta)}{\partial y}$ of the single "quasi"- Green's function (20) is problematic at $y = \eta$, where the derivative of $g_n(y, \eta)$ does not exist. Fortunately, we have the dual "quasi"- Green's function (22) to our disposal, from which we find that

$$\frac{\partial K(x, y, \xi, \eta)}{\partial y} = \frac{2\pi}{b^2}\sum_{n=1}^{\infty} n\, h_n(x, \xi)\cos\left(\frac{\pi n}{b}\eta\right)\sin\left(\frac{\pi n}{b}y\right)$$

The corresponding partial derivatives for the voltage are

$$\begin{cases} \frac{\partial V(x,y,x_{in},y_{in},x_{out},y_{out})}{\partial x} = \frac{2\pi}{a^2}\sum_{n=1}^{\infty} n\ \left(g_n\left(y,y_{in}\right)\cos\left(\frac{\pi n}{a}x_{in}\right) - g_n\left(y,y_{out}\right)\cos\left(\frac{\pi n}{a}x_{out}\right)\right)\sin\left(\frac{\pi n}{a}x\right) \\ \frac{\partial V(x,y,x_{in},y_{in},x_{out},y_{out})}{\partial y} = \frac{2\pi}{b^2}\sum_{n=1}^{\infty} n\ \left(h_n\left(x,x_{in}\right)\cos\left(\frac{\pi n}{b}y_{in}\right) - h_n\left(x,x_{out}\right)\cos\left(\frac{\pi n}{b}y_{out}\right)\right)\cos\left(\frac{\pi n}{b}y\right) \end{cases}$$

which specify the magnitude of current density

$$\left|j\left(x,y;\left(x_{in},y_{in}\right),\left(x_{out},y_{out}\right)\right)\right| = \sigma\sqrt{\left(\frac{\partial V\left(x,y,x_{in},y_{in},x_{out},y_{out}\right)}{\partial x}\right)^2 + \left(\frac{\partial V\left(x,y,x_{in},y_{in},x_{out},y_{out}\right)}{\partial y}\right)^2} \tag{26}$$

In contrast to the partial derivatives of the double Fourier series (12), the above single series converges considerably faster and can be used for numerical computations to compute the magnitude $|j\left(x,y\right)|$ of the current density. Perhaps, more importantly, our mathematical derivation is consistent with numerical computations of the magnitude $|j\left(x,y\right)|$ of the current density, demonstrating that the single Fourier series (20) returns precisely the same results as the double Fourier series (12).

Finally, the q-analogue computation (39) of (26) leads to the best accuracy with least computational effort as illustrated in Fig. 4. Fig. 4 shows that the q-series computation at the white lines, where the

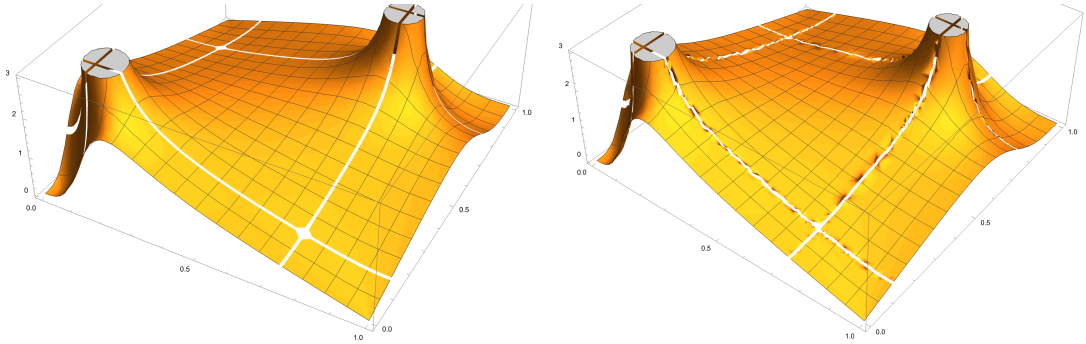


Figure 4: Again the same example computation that compares the single Fourier series (right) computation with the q-series (left). Only the $k = 0$ term in the series (38) gives the same "visual" (i.e. at least two digits) accuracy as evaluations with more terms (tested up to $k \leq K = 10$)!

derivative of $g_n\left(y,\eta\right)$ does not exist, leads to smooth lines. Precisely at these lines, the Fourier series converges badly (as shown in Section 4.3).

5 Summary

Our main result is the exact and efficient computation of the potential in (13), via the Green's function $K\left(x,y,\xi,\eta\right)$ expressed in (24) in terms of the q-function $T_q\left(x,y;\xi,\eta\right)$ in (25) and of the magnitude $|j(x,y)|$ of the current density in (26), where the derivatives $\frac{\partial K(x,y,\xi,\eta)}{\partial x}$ and $\frac{\partial K(x,y,\xi,\eta)}{\partial y}$ are computed by (39) together with the "q-series" (38), derived in Appendix D.2.

The astonishingly fast convergence of "q-series", in general, reduces the computation to only a few terms in the "q-series" (38). Even only one term, i.e. the $k = 0$ term, is used to produce Fig.

4 and visually no difference with more terms in the "q-series" (38) is observable. The $k = 0$ term approximation provides a simple, closed analytic formula, which is practical for quick estimates (of a quantities that are otherwise computationally very expensive).

Finally, we also include a drawing in Fig. 5 of the magnitude $|j(x, y)|$ in (26), computed with (39) and one term $k = 0$ in the "q-series" (38), for different source-destination pairs (s, d).

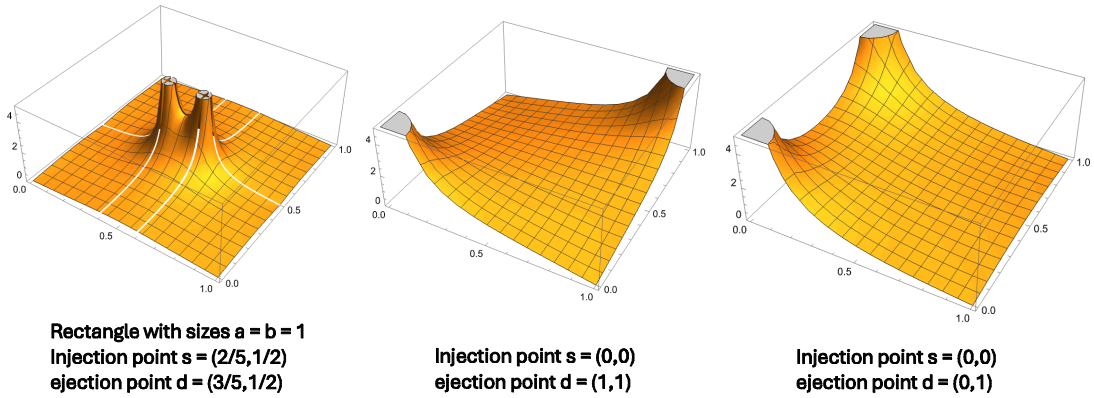


Figure 5: The magnitude $|j(x, y)|$ in (26), computed with (39) and one term $k = 0$ in the "q-series" (38), for different source-destination pairs (s, d).

Acknowledgement

I am very grateful to Wim van Horsen for his expert views and suggestions on the mathematical derivations. I am supported by the European Research Council (ERC) under the European Union's Horizon 2020 research and innovation programme (grant agreement No 101019718).

References

[1] L. Onsager. Crystal statistics: A two-dimensional model with an order-disorder transition. *Physical Review*, 65(3 and 4):117–149, February 1944.

[2] M. Kitsak, A. Ganin, A. Elmokashfi, H. Cui, D. A. Eisenberg, D. L. Alderson, D. Korkin, and I. Linkov. Finding shortest and nearly shortest path nodes in large substantially incomplete networks by hyperbolic mapping. *Nature Communications*, 14(186), https://doi.org/10.1038/s41467-022-35181-w, 2023.

[3] M. Raftopoulou, R. Litjens, and P. Van Mieghem. Fréchet distribution in geometric graphs for drone networks. *Physical Review E*, 106(2):024301, 2022.

[4] P. Van Mieghem. *Graph Spectra for Complex Networks*. Cambridge University Press, Cambridge, U.K., 2nd edition, 2023.

[5] K. Devriendt and P. Van Mieghem. The Simplex Geometry of Graphs. *Journal of Complex Networks*, 7(4):469–490, August 2019.

[6] R. P. Feynman, R. B. Leighton, and M. Sands. *The Feynman Lectures on Physics*, volume 2. Addison-Wesley, Massachusetts, 1963.

[7] E. C. Titchmarsh. *The Theory of Functions*. Oxford University Press, Amen House, London, 1964.

[8] R. Courant and D. Hilbert. *Methods of Mathematical Physics*, volume I of *Wiley Classic Library*. Interscience, New York, first english edition, translated and revised from the german original of springer in 1937 edition, 1953.

[9] E. Zauderer. *Partial Differential Equations of Applied Mathematics*. John Wiley & Sons, 1983.

[10] P. Van Mieghem. *The Mittag-Leffler and Gamma function*. Oxford Mathematical Monographs. Oxford University Press, 2026.

[11] E. C. Titchmarsh and D. R. Heath-Brown. *The Theory of the Zeta-function*. Oxford Science Publications, Oxford, 2nd edition, 1986.

[12] P. M. Morse and H. Feshbach. *Methods of Theoretical Physics*. McGraw-Hill Book Company, New York, 1978.

[13] G. F. D. Duff and D. Naylor. *Differential Equations of Applied Mathematics*. John Wiley & Sons, 1966.

[14] J. Tannery and J. Molk. *Éléments de la Théorie des Functions Elliptiques*. Thome II. Gauthier-Villars et fils, Paris, 1896.

[15] G. Sansone and J. Gerretsen. *Lectures on the Theory of Functions of a Complex Variable*, volume 1 and 2. P. Noordhoff, Groningen, 1960.

[16] P. Van Mieghem. The arithmetic-geometric mean: A pearl of Gauss. *Delft University of Technology, report20230605*, 2023.

[17] K. Chandrasekharan. *Elliptic Functions*. Springer-Verlag, Berlin, 1985.

[18] H. Rademacher. *Topics in Analytic Number Theory*. Springer-Verlag, Berlin, 1973.

[19] I. P. Goulden and D. M. Jackson. *Combinatorial Enumeration*. John Wiley & Sons, New York, 1983.

[20] G. E. Andrews. *The Theory of Partitions*. Cambridge University Press, Cambridge, U.K., 1998.

[21] G. H. Hardy and E. M. Wright. *An Introduction to the Theory of Numbers*. Oxford University Press, London, 6th edition, 2008.

[22] G. E. Andrews. *q-series: Their development and application in analysis, number theory, combinatorics, physics and computer algebra*, volume Conference Board of the Mathematical Sciences, Regional Conference Series in Mathematics of *66*. American Mathematical Society, Providence, Rhode Island, 1986.

[23] M. Abramowitz and I. A. Stegun. *Handbook of Mathematical Functions*. Dover Publications, Inc., New York, 1968.

A Elements from Fourier theory

A.1 Orthogonality properties

The well-known orthogonality property in the theory of Fourier series is

$$\int_0^\pi \cos m\theta \cos k\theta d\theta = 0 \quad \text{for } k \neq m$$

and

$$\int_0^\pi \cos^2 k\theta d\theta = \pi 1_{\{k=0\}} + \frac{\pi}{2} 1_{\{k\neq 0\}}$$

as well as

$$\begin{cases} \int_0^\pi \sin m\theta \sin k\theta d\theta = 0 & \text{for } k \neq m \\ \int_{-\pi}^\pi \sin^2 k\theta d\theta = \pi \end{cases}$$

and $\int_{-\pi}^\pi \sin m\theta \cos k\theta d\theta = 0$.

Indeed, with $\cos m\theta \cos k\theta = \frac{1}{2}\cos(m-k)\theta + \frac{1}{2}\cos(m+k)\theta$, it holds that

$$\begin{aligned} \int_0^\pi \cos m\theta \cos k\theta d\theta &= \frac{1}{2}\int_0^\pi \cos(m-k)\theta d\theta + \frac{1}{2}\int_0^\pi \cos(m+k)\theta d\theta \\ &= \frac{1}{2}\frac{\sin(m-k)\pi}{(m-k)} + \frac{1}{2}\frac{\sin(m+k)\pi}{(m+k)} \end{aligned}$$

which vanishes if $k \neq m$, but $\lim_{m\to k} \frac{1}{2}\frac{\sin(m-k)\pi}{(m-k)} = \frac{\pi}{2}$, except if $m = k = 0$. The other integrals similarly follow from $\sin m\theta \sin k\theta = \frac{1}{2}\cos(m-k)\theta - \frac{1}{2}\cos(m+k)\theta$.

A.2 The Fourier series $S(x) = \sum_{m=1}^{\infty} \frac{\sin xm}{m}$

The sum $S(x) = \sum_{m=1}^{\infty} \frac{\sin xm}{m} = \operatorname{Im} \sum_{m=1}^{\infty} \frac{\left(e^{ix}\right)^m}{m}$ is periodic in the real x with periodic 2π. Clearly, $S(0) = S(\pi) = 0$. Since the Taylor series $\sum_{m=1}^{\infty} \frac{z^m}{m} = -\log(1-z)$ converges for $|z| \leq 1$, except for the point $z = 1$, it holds, for $0 < x < 2\pi$, that

$$\sum_{m=1}^{\infty} \frac{e^{ixm}}{m} = -\log\left(1 - e^{ix}\right)$$

from which $S(x) = \operatorname{Im} \sum_{m=1}^{\infty} \frac{\left(e^{ix}\right)^m}{m} = -\operatorname{Im} \log\left(1 - e^{ix}\right)$.

Now,

$$\begin{aligned} 1 - e^{ix} &= 1 - \cos x - i \sin x = \sqrt{(1-\cos x)^2 + \sin^2 x} e^{-i \arctan \frac{\sin x}{1-\cos x}} \\ &= \sqrt{2 - 2\cos x} e^{-i \arctan \frac{2 \sin \frac{x}{2} \cos \frac{x}{2}}{2 - 2\cos^2 \frac{x}{2}}} = \sqrt{2\left(1 - \left(1 - 2\sin^2 \frac{x}{2}\right)\right)} e^{-i \arctan \frac{\cos \frac{x}{2}}{\sin \frac{x}{2}}} \\ &= 2\left|\sin \frac{x}{2}\right| e^{-i \arctan \frac{1}{\tan \frac{x}{2}}} \end{aligned}$$

With

$$\arctan x + \arctan \frac{1}{x} = \lim_{z_2 \to \frac{1}{x}} \arctan\left(\frac{x + \frac{1}{x}}{1 - x z_2}\right) = \begin{cases} \frac{\pi}{2} & \text{for } x \geq 0 \\ -\frac{\pi}{2} & \text{for } x < 0 \end{cases}$$

and the function $\operatorname{sign}(x) = 1$ if $x \geq 0$, else $\operatorname{sign}(x) = -1$, we find that

$$\log\left(1 - e^{ix}\right) = \log\left(2\left|\sin \frac{x}{2}\right| e^{-i\left(\frac{\pi}{2}\operatorname{sign}(x) - \frac{A}{2}\right)}\right) = \log\left(2\left|\sin \frac{x}{2}\right|\right) - i\left(\frac{\pi}{2}\operatorname{sign}(x) - \frac{x}{2}\right)$$

Separating real and imaginary part in $\sum_{m=1}^{\infty} \frac{e^{ixm}}{m} = -\log\left(1 - e^{ix}\right)$ shows, for $0 \leq x \leq 2\pi$, that

$$S(x) = \sum_{m=1}^{\infty} \frac{\sin xm}{m} = \frac{\pi}{2}\operatorname{sign}(x) - \frac{x}{2}$$

while, for $0 < x < 2\pi$,

$$\sum_{m=1}^{\infty} \frac{\cos xm}{m} = -\log\left(2\left|\sin \frac{x}{2}\right|\right) \tag{27}$$

Both the sine and cosine Fourier series converge very slowly, due to their close proximity to the diverging harmonic series for $x = 0$ in $\sum_{m=1}^{\infty} \frac{\cos xm}{m} = \lim_{N\to\infty} \sum_{m=1}^{N} \frac{1}{m}$, where $H_N = \sum_{m=1}^{N} \frac{1}{m}$ is the harmonic series, discussed in [10, Part II]. This type of very slowly converging series occurs in the current density derived from the double Fourier series (30).

B Green's function in 2D

The idea of Green's function (or influence function [8, §14, p. 351]) stems from the linearity of the Poisson equation $\Delta V = -\varphi(r)$, where r denotes the vector in D dimensions. If the density of charges $\varphi(r)$ is "piecewise continuous", then $\varphi(r)$ can be decomposed as a continuous sum over point charges. Suppose that $K(r, r_p)$ is a solution of the Poisson equation

$$\Delta K(r, r_p) = -\delta(r - r_p) \tag{28}$$

with same boundary conditions are in the original problem, then

$$V(r) = \int_{vol} \varphi(r_p) K(r, r_p) dr_p \tag{29}$$

where *vol* is the region in D dimension containing the charges, formally (but proved in [8, p. 353-354]) obeys the Poisson equation $\Delta V = -\varphi(r)$, because

$$\Delta V(r) = \int_{vol} \varphi(r_p) \Delta K(r, r_p) dr_p = -\int_{vol} \varphi(r_p) \delta(r - r_p) dr_p = -\varphi(r)$$

The function $K(r, r_p)$ is called the influence or Green's function. The theory of Green's function is rich, see e.g. [9, Chapter 7], [12, Chapter 7], [13]. The symmetry relation $K(r, r_p) = K(r_p, r)$ is key.

Another building block in the theory of Green's functions are eigenfunctions of the differential equation $\Delta V(r) + \alpha V(r) = -\varphi(r)$. Let the eigenfunction $u_m(r)$ obey $\Delta u_m(r) = \lambda_m w'(r) u_m(r)$ as well as the boundary conditions, where $w(r)$ is the associated, positive weight function [4, art 350] with derivative $w'(r)$ that defines the scalar product

$$(f, g) = \int_{vol} f(r) g(r) dw(r)$$

and orthogonality among eigenfunctions $(u_m, u_k) = \delta_{km}$. Courant & Hilbert [8, p. 360] show that the eigenfunctions $\{u_m(r)\}_{m \geq 1}$ form a complete orthogonal set. Hence, the Green's function can be written as a linear combination of eigenfunctions,

$$K(r, r_p) = \sum_{m=1}^{\infty} c_m u_m(r)$$

where $c_m = (K(r, r_p), u_m(r)) = \int_{vol} K(r, r_p) u_m(r) dw(r)$. Multiplying $\Delta K(r, r_p) = -\delta(r - r_p)$ by $u_k(r)$ and integrating over the region

$$\int_{vol} u_k(r) \Delta K(r, r_p) dr = -\int_{vol} u_k(r) \delta(r - r_p) dr = -u_k(r_p)$$

yields, with $K(r, r_p) = \sum_{m=1}^{\infty} c_m u_m(r)$, $\Delta u_m(r) = \lambda_m \frac{dw(r)}{dr} u_m(r)$ and $(u_m, u_k) = \delta_{km}$,

$$-u_k(r_p) = \int_{vol} u_k(r) \sum_{m=1}^{\infty} c_m \Delta u_m(r) d(r) = \sum_{m=1}^{\infty} c_m \lambda_m \int_{vol} u_k(r) u_m(r) dw(r) = c_k \lambda_k$$

leading to $c_k = -\frac{u_k(r_p)}{\lambda_k}$. Hence, we arrive at the eigenfunction expansion of the Green's function

$$K(r, r_p) = -\sum_{m=1}^{\infty} \frac{u_m(r_p) u_m(r)}{\lambda_m}$$

which demonstrates symmetry $K(r, r_p) = K(r_p, r)$ between observer at the point r and the point charge at point r_p.

B.1 Examples

Morse and Feshbach [12] shows that, for large sizes a and b the rectangle, the Green's function should behave as $K\left(x,y;x_{in},y_{in}\right)\approx -2\log\left(\sqrt{\left(x-x_{in}\right)^2+\left(y-y_{in}\right)^2}\right)$.

Zauderer [9, Example 5, p. 389-392] presents the solution of

$$\frac{\partial^2 K}{\partial x^2}+\frac{\partial^2 K}{\partial y^2}=-\delta\left(x_{\,in},y_{in}\right)=-\delta\left(x-\xi\right)\delta\left(y-\eta\right)$$

with Dirichlet boundary conditions $V=0$ at the boundary of the rectangle $\left(0,0\right),\left(0,b\right),\left(a,b\right)$ and $\left(a,0\right)$. There are two representations,

$$K\left(x,y;\xi,\eta\right)=\frac{4}{ab}\sum_{n=1}^{\infty}\sum_{m=1}^{\infty}\frac{\sin\left(\frac{\pi n}{a}x\right)\sin\left(\frac{\pi n}{a}\xi\right)\sin\left(\frac{\pi m}{b}y\right)\sin\left(\frac{\pi m}{b}\eta\right)}{\left(\frac{\pi n}{a}\right)^2+\left(\frac{\pi m}{b}\right)^2}$$

and the faster converging series [12, p. 800]

$$K\left(x,y;\xi,\eta\right)=\frac{2}{\pi}\sum_{k=1}^{\infty}\frac{\sin\left(\frac{\pi k}{a}x\right)\sin\left(\frac{\pi k}{a}\xi\right)}{k\sinh\left(\frac{\pi k}{a}b\right)}q_k\left(y\right)$$

with

$$q_k\left(y\right)=\begin{cases}\sinh\left(\frac{\pi k}{a}y\right)\sinh\left(\frac{\pi k}{a}\left(b-\eta\right)\right) & \eta>y\\ \sinh\left(\frac{\pi k}{a}\eta\right)\sinh\left(\frac{\pi k}{a}\left(b-y\right)\right) & \eta<y\end{cases}$$

The solution [9, p. 399], [13, p. 281] of

$$\frac{\partial^2 K}{\partial x^2}+\frac{\partial^2 K}{\partial y^2}=-\delta\left(x_{\,in},y_{in}\right)=-\delta\left(x-\xi\right)\delta\left(y-\eta\right)$$

with Neumann boundary conditions $\frac{\partial V}{\partial n}=0$ at the boundary of the rectangle $\left(0,0\right),\left(0,b\right),\left(a,b\right)$ and $\left(a,0\right)$ is

$$\begin{aligned}K\left(x,y;\xi,\eta\right)=&\frac{2}{ab}\sum_{n=1}^{\infty}\frac{\cos\left(\frac{\pi n}{a}x\right)\cos\left(\frac{\pi n}{a}\xi\right)}{\left(\frac{\pi n}{a}\right)^2}+\frac{2}{ab}\sum_{m=1}^{\infty}\frac{\cos\left(\frac{\pi m}{b}y\right)\cos\left(\frac{\pi m}{b}\eta\right)}{\left(\frac{\pi m}{b}\right)^2}\\&+\frac{4}{ab}\sum_{n=1}^{\infty}\sum_{m=1}^{\infty}\frac{\cos\left(\frac{\pi n}{a}x\right)\cos\left(\frac{\pi n}{a}\xi\right)\cos\left(\frac{\pi m}{b}y\right)\cos\left(\frac{\pi m}{b}\eta\right)}{\left(\frac{\pi n}{a}\right)^2+\left(\frac{\pi m}{b}\right)^2}\end{aligned}\tag{30}$$

which is associated to (10) in 3D with current injection as $K\left(x,y;x_{in},y_{in}\right)-K\left(x,y;x_{out},y_{out}\right)$. The shorter notation as a double Fourier series of (30) in [13, p. 281] is

$$K\left(x,y;\xi,\eta\right)=\frac{4}{ab}\sum_{n=0}^{\infty}\sum_{m=0}^{\infty}\gamma_{nm}\frac{\cos\left(\frac{\pi n}{a}x\right)\cos\left(\frac{\pi n}{a}\xi\right)\cos\left(\frac{\pi m}{b}y\right)\cos\left(\frac{\pi m}{b}\eta\right)}{\left(\frac{\pi n}{a}\right)^2+\left(\frac{\pi m}{b}\right)^2}\tag{31}$$

with $\gamma_{00}=0$, $\gamma_{0m}=\gamma_{n0}=\frac{1}{2}$ and $\gamma_{nm}=1$ for $n>0$ and $m>0$. Unfortunately, it seems that a single and faster converging series as for the boundary conditions $V=0$ above is not available, which has motivated our computation in Section 4.2.

B.2 Polar coordinates

The Laplacian operator in polar coordinates, $x = r\cos\varphi$ and $y = r\sin\varphi$, is[10]

$$\frac{\partial^2}{\partial x^2} + \frac{\partial^2}{\partial y^2} = \frac{\partial^2}{\partial r^2} + \frac{1}{r}\frac{\partial}{\partial r} + \frac{1}{r^2}\frac{\partial^2}{\partial \varphi^2} \tag{32}$$

The solution of

$$\frac{\partial^2 V(r,\varphi)}{\partial r^2} + \frac{1}{r}\frac{\partial V(r,\varphi)}{\partial r} + \frac{1}{r^2}\frac{\partial^2 V(r,\varphi)}{\partial \varphi^2} = 0$$

with separation of coordinates $V(r,\varphi) = R(r)F(\varphi)$ becomes

$$R''(r)F(\varphi) + \frac{1}{r}R'(r)F(\varphi) + \frac{1}{r^2}R(r)F''(\varphi) = 0$$

Dividing by $V(r,\varphi) = R(r)F(\varphi) > 0$ and multiplying by r^2 yields

$$r^2\frac{R''(r)}{R(r)} + r\frac{R'(r)}{R(r)} + \frac{F''(\varphi)}{F(\varphi)} = 0$$

The separate differentiations

$$\begin{cases} \frac{d}{dr}\left(r^2\frac{R''(r)}{R(r)} + r\frac{R'(r)}{R(r)}\right) = 0 \\ \frac{d}{d\varphi}\frac{F''(\varphi)}{F(\varphi)} = 0 \end{cases}$$

lead, after integration, to

$$\begin{cases} r^2\frac{R''(r)}{R(r)} + r\frac{R'(r)}{R(r)} = \lambda_r \\ \frac{F''(\varphi)}{F(\varphi)} = \lambda_\varphi \end{cases}$$

where the integration constants satisfy $\lambda_r + \lambda_\varphi = 0$. The differential equation $r^2R''(r) + rR'(r) = \lambda_r R(r)$ transforms with $\frac{d}{dr}(rR'(r)) = rR''(r) + R'(r)$ to $\frac{d}{dr}(rR'(r)) = \frac{\lambda_r}{r}R(r)$. Further progress requires the boundary conditions.

The governing equation (28) of Green's function becomes

$$\frac{\partial^2 K(r,\varphi)}{\partial r^2} + \frac{1}{r}\frac{\partial K(r,\varphi)}{\partial r} + \frac{1}{r^2}\frac{\partial^2 K(r,\varphi)}{\partial \varphi^2} = -\frac{1}{r}\delta(r - r_s)\,\delta(\varphi - \varphi_s)$$

because $1 = \int_{-\infty}^{\infty} dx \int_{-\infty}^{\infty} dy \delta(x - x_s)\,\delta(y - y_s) = \int_0^{\infty} r dr \int_0^{2\pi} \delta\varphi \left(\frac{1}{r}\delta(r - r_s)\right)\delta(\varphi - \varphi_s)$. If $K(r,\varphi)$ operates in the entire 2D plane, then Duff and Naylor [13, Sec. 7.2] argue that, by symmetry, the Green's function $K(r,\varphi)$ will only depend upon r, the distance of source and observer. If the source is at the origin, they pose

$$\frac{d^2K(r)}{dr^2} + \frac{1}{r}\frac{dK(r)}{dr} = -\frac{1}{2\pi r}\delta(r) \tag{33}$$

which reduces to

$$-\frac{1}{2\pi}\delta(r) = r\frac{d^2K(r)}{dr^2} + \frac{dK(r)}{dr} = \frac{d}{dr}\left(r\frac{dK(r)}{dr}\right)$$

[10] A tedious computation of the chain rule, starting with

$$\frac{\partial}{\partial r} = \frac{\partial}{\partial x}\frac{\partial x}{\partial r} + \frac{\partial}{\partial y}\frac{\partial y}{\partial r} = \frac{\partial}{\partial x}\cos\varphi + \frac{\partial}{\partial y}\sin\varphi$$
$$\frac{\partial}{\partial \varphi} = \frac{\partial}{\partial x}\frac{\partial x}{\partial \varphi} + \frac{\partial}{\partial y}\frac{\partial y}{\partial \varphi} = -r\frac{\partial}{\partial x}\sin\varphi + r\frac{\partial}{\partial y}\cos\varphi$$

finally leads to (32)..

Integrating both sides from 0 to r yields, with $\lim_{r\to 0} r\frac{dK(r)}{dr} = c$, to $r\frac{dK(r)}{dr} - c = -\frac{1}{2\pi}$ or

$$\frac{dK(r)}{dr} = \frac{c - \frac{1}{2\pi}}{r}$$

Another integration leads, with $\widetilde{c} = c - \frac{1}{2\pi}$, to

$$K(r) = \widetilde{c}\log r + K(1) \tag{34}$$

Duff and Naylor [13, Sec. 7.2] give the particular solution $K(r) = -\frac{1}{2\pi}\log r$ and remark that $\lim_{r\to\infty} K(r) = -\infty$ in 2D, rather than 0 as in 3D.

B.3 Conformal mapping

Duff and Naylor [13, p. 271] invoke conformal mapping $w = f(z)$ that maps a region D into the unit circle $|w| < 1$, with a given source point s being mapped into the origin $w = 0$ of the circle such that $f(z_s) = 0$ and $f'(z_s) \neq 0$. The Green's function of the region D is

$$K(x, y) = \widetilde{c}\log|f(x + iy)| = \widetilde{c}\,\mathrm{Re}(\log f(z)) \tag{35}$$

Indeed, the real (or/and imaginary) part of an analytic function is, by the Cauchy-Riemann equations, an harmonic functions satisfying the Laplacian. At the point $z_s = x_s + iy_s$, the Green's function $K(x_s, y_s)$ has a logarithmic singularity and satisfies the Poisson equation (28) as demonstrated by (34). Also, a point (x, y) on the boundary ∂D of the region D is mapped to a point $|w| = 1$ on the unit circle, for which $K(x, y) = 0$, thus, satisfying the Dirichlet boundary conditions. As an example, Duff and Naylor [13, p. 271] consider as the region D, a unit circle and the Möbius map $w = \frac{z - z_s}{z_s^* z - 1}$, where the complex conjugate $z_s^* = x_s - iy_s$, maps the disk $|z| \leq 1$ into the unit disk $|w| \leq 1$ where z_s is mapped to the origin. Hence, the Green's function (35) becomes

$$K(x, y; x_s, y_s) = \widetilde{c}\log\left|\frac{z - z_s}{z_s^* z - 1}\right|$$

In the same vein, Courant and Hilbert [8, p. 384-386] illustrate a beautiful elliptic solution (in terms of Weierstrass's σ- function) of the two dimension partial differential equation (28) with Dirichlet boundary conditions $V = 0$ on the boundary of the rectangle, which transforms via the Cauchy-Riemann equations to analytic functions in the complex plane.

Our q-series solution (24) together with (25) is a similar example for the Neumann boundary conditions and quasi-Green's functions (that require two opposite delta functions).

C Theta-function evaluation of the Green's function (30)

After using $\frac{1}{s} = \int_0^\infty e^{-st}dt$ for $\mathrm{Re}(s) > 0$, the Green's function (30) is transformed into

$$K(x, y; \xi, \eta) = \frac{2}{ab}\int_0^\infty \sum_{n=1}^{\infty} \cos\left(\frac{\pi n}{a}x\right)\cos\left(\frac{\pi n}{a}\xi\right) e^{-\left(\frac{\pi n}{a}\right)^2 t}dt + \frac{2}{ab}\int_0^\infty \sum_{m=1}^{\infty} \cos\left(\frac{\pi m}{b}y\right)\cos\left(\frac{\pi m}{b}\eta\right) e^{-\left(\frac{\pi m}{b}\right)^2 t}dt$$
$$+ \frac{4}{ab}\int_0^\infty \sum_{n=1}^{\infty} \cos\left(\frac{\pi n}{a}x\right)\cos\left(\frac{\pi n}{a}\xi\right) e^{-\left(\frac{\pi n}{a}\right)^2 t} \sum_{m=1}^{\infty} \cos\left(\frac{\pi m}{b}y\right)\cos\left(\frac{\pi m}{b}\eta\right) e^{-\left(\frac{\pi m}{b}\right)^2 t}dt$$

We write

$$\sum_{n=1}^{\infty}\cos\left(\frac{\pi n}{a}x\right)\cos\left(\frac{\pi n}{a}\xi\right)e^{-\left(\frac{\pi n}{a}\right)^2 t}=\mathrm{Re}\left(\sum_{n=1}^{\infty}\left(e^{i\frac{\pi}{a}(x+\xi)}\right)^n e^{-\left(\frac{\pi n}{a}\right)^2 t}+\sum_{n=1}^{\infty}\left(e^{i\frac{\pi}{a}(x-\xi)}\right)^n e^{-\left(\frac{\pi n}{a}\right)^2 t}\right)$$

The appearing series $\sum_{n=1}^{\infty} z^n e^{-\left(\frac{\pi n}{a}\right)^2 t}$ can be reformulated in terms of the theta $\theta_3\left(z|\tau\right)=\sum_{m=-\infty}^{\infty} q^{m^2} e^{2m\pi i z}$ function [14, art. 160] with $q=e^{\pi i\tau}$ and $\mathrm{Im}\left(\tau\right)>0$, also written as $\theta_3\left(z|\tau\right)=1+2\sum_{m=1}^{\infty} q^{m^2}\cos\left(2m\pi z\right)$, as

$$\begin{aligned}\sum_{n=1}^{\infty}\cos\left(\frac{\pi n}{a}x\right)\cos\left(\frac{\pi n}{a}\xi\right)e^{-\left(\frac{\pi n}{a}\right)^2 t}&=\sum_{n=1}^{\infty}\cos\left(\frac{\pi n}{a}\left(x+\xi\right)\right)e^{-\left(\frac{\pi n}{a}\right)^2 t}+\sum_{n=1}^{\infty}\cos\left(\frac{\pi n}{a}\left(x-\xi\right)\right)e^{-\left(\frac{\pi n}{a}\right)^2 t}\\&=\frac{1}{2}\left(\theta_3\left(\frac{(x+\xi)}{2a}\middle| i\frac{\pi}{a^2}t\right)+\theta_3\left(\frac{(x-\xi)}{2a}\middle| i\frac{\pi}{a^2}t\right)\right)-1\end{aligned}$$

Thus, $q=e^{-\left(\frac{\pi}{a}\right)^2 t}$. After simplification, where the constant term -1 disappeared, we find that

$$\begin{aligned}K\left(x,y;\xi,\eta\right)=&-\frac{1}{ab}\int_0^{\infty}\left(\theta_3\left(\frac{(x+\xi)}{2a}\middle| i\frac{\pi}{a^2}t\right)+\theta_3\left(\frac{(x-\xi)}{2a}\middle| i\frac{\pi}{a^2}t\right)\right)dt\\&-\frac{1}{ab}\int_0^{\infty}\left(\theta_3\left(\frac{(y+\eta)}{2b}\middle| i\frac{\pi}{b^2}t\right)+\theta_3\left(\frac{(y-\eta)}{2b}\middle| i\frac{\pi}{b^2}t\right)\right)dt\\&+\frac{1}{ab}\int_0^{\infty}\left(\theta_3\left(\frac{(x+\xi)}{2a}\middle| i\frac{\pi}{a^2}t\right)+\theta_3\left(\frac{(x-\xi)}{2a}\middle| i\frac{\pi}{a^2}t\right)\right)\\&\times\left(\theta_3\left(\frac{(y+\eta)}{2b}\middle| i\frac{\pi}{b^2}t\right)+\theta_3\left(\frac{(y-\eta)}{2b}\middle| i\frac{\pi}{b^2}t\right)\right)dt\end{aligned}\tag{36}$$

This theta function approach (36) may be regarded as the more fundamental, because a rectangle can be transformed into a half-plane by an elliptic function (see e.g. [15]). Any elliptic function can be written in terms of the four theta functions. The theory of elliptic functions is a pearl of complex function theory, established in the 19-th century, starting with Gauss's work on the arithmetic-geometric mean [16], followed by Abel, Jacobi, Weierstrass and others.

Although exact, (36) requires the integral over all positive t. Numerically, we found that contour plots computed from (36) with Mathematica were computationally (i.e. in time) demanding. In addition, the partial derivatives with respect to x and y are not straightforwardly written in terms of the four theta-function. Therefore, we have not further exploited (36).

D Evaluation of the single sum quasi-Green's function (22)

D.1 Voltage: Single sum quasi-Green's function (22)

We confine ourselves to the single sum quasi-Green's function (22) in the interval $0\leq\eta\leq y$, where (21) indicates that

$$K\left(x,y,\xi,\eta\right)=\frac{1}{a}g_0\left(y,\eta\right)+\frac{2}{\pi}\sum_{n=1}^{\infty}\frac{\cosh\frac{\pi n}{a}\left(b-y\right)\cosh\frac{\pi n}{a}\eta}{n\sinh\left(\frac{\pi n}{a}b\right)}\cos\left(\frac{\pi n}{a}\xi\right)\cos\left(\frac{\pi n}{a}x\right)$$

After invoking $2\cos a\cos b=\cos\left(a+b\right)+\cos\left(a-b\right)$, the n-sum is

$$\begin{aligned}S=&\frac{1}{\pi}\sum_{n=1}^{\infty}\frac{\cosh\frac{\pi n}{a}\left(b-y\right)\cosh\frac{\pi n}{a}\eta}{n\sinh\left(\frac{\pi n}{a}b\right)}\cos\left(\frac{\pi n}{a}\left(\xi+x\right)\right)\\&+\frac{1}{\pi}\sum_{n=1}^{\infty}\frac{\cosh\frac{\pi n}{a}\left(b-y\right)\cosh\frac{\pi n}{a}\eta}{n\sinh\left(\frac{\pi n}{a}b\right)}\cos\left(\frac{\pi n}{a}\left(\xi-x\right)\right)\end{aligned}$$

Similarly, with $2\cosh a\cosh b=\cosh\left(a+b\right)+\cosh\left(a-b\right)$, we have that

$$\begin{aligned}S=&\frac{1}{2\pi}\sum_{n=1}^{\infty}\frac{\cosh\frac{\pi n}{a}\left(b-y+\eta\right)}{n\sinh\left(\frac{\pi n}{a}b\right)}\cos\left(\frac{\pi n}{a}\left(\xi+x\right)\right)+\\&+\frac{1}{2\pi}\sum_{n=1}^{\infty}\frac{\cosh\frac{\pi n}{a}\left(b-y-\eta\right)}{n\sinh\left(\frac{\pi n}{a}b\right)}\cos\left(\frac{\pi n}{a}\left(\xi+x\right)\right)\\&+\frac{1}{2\pi}\sum_{n=1}^{\infty}\frac{\cosh\frac{\pi n}{a}\left(b-y+\eta\right)}{n\sinh\left(\frac{\pi n}{a}b\right)}\cos\left(\frac{\pi n}{a}\left(\xi-x\right)\right)\\&+\frac{1}{2\pi}\sum_{n=1}^{\infty}\frac{\cosh\frac{\pi n}{a}\left(b-y-\eta\right)}{n\sinh\left(\frac{\pi n}{a}b\right)}\cos\left(\frac{\pi n}{a}\left(\xi-x\right)\right)\end{aligned}$$

Finally, with $\cosh a=\cos ia$, we find the reduction

$$\begin{aligned}S=&\frac{1}{4\pi}\sum_{n=1}^{\infty}\frac{\cos\frac{\pi n}{a}\left(\left(\xi+x\right)+i\left(b-y+\eta\right)\right)}{n\sinh\left(\frac{\pi n}{a}b\right)}+\frac{1}{4\pi}\sum_{n=1}^{\infty}\frac{\cos\frac{\pi n}{a}\left(\left(\xi+x\right)-i\left(b-y+\eta\right)\right)}{n\sinh\left(\frac{\pi n}{a}b\right)}\\&+\frac{1}{4\pi}\sum_{n=1}^{\infty}\frac{\cos\frac{\pi n}{a}\left(\left(\xi+x\right)+i\left(b-y-\eta\right)\right)}{n\sinh\left(\frac{\pi n}{a}b\right)}+\frac{1}{4\pi}\sum_{n=1}^{\infty}\frac{\cos\frac{\pi n}{a}\left(\left(\xi+x\right)-i\left(b-y-\eta\right)\right)}{n\sinh\left(\frac{\pi n}{a}b\right)}\\&+\frac{1}{4\pi}\sum_{n=1}^{\infty}\frac{\cos\frac{\pi n}{a}\left(\left(\xi-x\right)+i\left(b-y+\eta\right)\right)}{n\sinh\left(\frac{\pi n}{a}b\right)}+\frac{1}{4\pi}\sum_{n=1}^{\infty}\frac{\cos\frac{\pi n}{a}\left(\left(\xi-x\right)-i\left(b-y+\eta\right)\right)}{n\sinh\left(\frac{\pi n}{a}b\right)}\\&+\frac{1}{4\pi}\sum_{n=1}^{\infty}\frac{\cos\frac{\pi n}{a}\left(\left(\xi-x\right)+i\left(b-y-\eta\right)\right)}{n\sinh\left(\frac{\pi n}{a}b\right)}+\frac{1}{4\pi}\sum_{n=1}^{\infty}\frac{\cos\frac{\pi n}{a}\left(\left(\xi-x\right)-i\left(b-y-\eta\right)\right)}{n\sinh\left(\frac{\pi n}{a}b\right)}\end{aligned}$$

With $\cos x=\frac{e^{ix}+e^{-ix}}{2}=\mathrm{Re}\left(e^{ix}\right)$ and $A=\frac{\pi b}{a}$, each of the sums is of the type

$$w\left(z,A\right)=\sum_{n=1}^{\infty}\frac{z^{n}}{n\sinh\left(An\right)}=2\sum_{n=1}^{\infty}\frac{z^{n}}{n\left(e^{An}-e^{-An}\right)}\tag{37}$$

with $w\left(0,A\right)=0$. Thus, the single sum quasi-Green's function (22) in the interval $0\leq\eta\leq y$ is represented as

$$\begin{aligned}K\left(x,y,\xi,\eta\right)=&\frac{1}{a}g_{0}\left(y,\eta\right)+\frac{\mathrm{Re}\left\{w\left(e^{i\frac{\pi}{a}\left(\xi+x\right)}e^{-\frac{\pi}{a}\left(b-y+\eta\right)},\frac{\pi b}{a}\right)+w\left(e^{i\frac{\pi}{a}\left(\xi+x\right)}e^{\frac{\pi}{a}\left(b-y+\eta\right)},\frac{\pi b}{a}\right)\right\}}{4\pi}\\&+\frac{\mathrm{Re}\left\{w\left(e^{i\frac{\pi}{a}\left(\xi+x\right)}e^{-\frac{\pi}{a}\left(b-y-\eta\right)},\frac{\pi b}{a}\right)+w\left(e^{i\frac{\pi}{a}\left(\xi+x\right)}e^{\frac{\pi}{a}\left(b-y-\eta\right)},\frac{\pi b}{a}\right)\right\}}{4\pi}\\&+\frac{\mathrm{Re}\left\{w\left(e^{i\frac{\pi}{a}\left(\xi-x\right)}e^{-\frac{\pi}{a}\left(b-y+\eta\right)},\frac{\pi b}{a}\right)+w\left(e^{i\frac{\pi}{a}\left(\xi-x\right)}e^{\frac{\pi}{a}\left(b-y+\eta\right)},\frac{\pi b}{a}\right)\right\}}{4\pi}\\&+\frac{\mathrm{Re}\left\{w\left(e^{i\frac{\pi}{a}\left(\xi-x\right)}e^{-\frac{\pi}{a}\left(b-y-\eta\right)},\frac{\pi b}{a}\right)+w\left(e^{i\frac{\pi}{a}\left(\xi-x\right)}e^{\frac{\pi}{a}\left(b-y-\eta\right)},\frac{\pi b}{a}\right)\right\}}{4\pi}\end{aligned}$$

where the function $w(z,A)$ is studied in Appendix F.

In the sequel, we simplify the real part and present, perhaps, the simplest possible form in (25) below. With $w(z,A) = -2\log\prod_{k=0}^{\infty}\left(1-ze^{-A}q^k\right)$ and $q = e^{-2A}$ in (52), taking into account that $0 \le \eta \le y$,

$$\begin{aligned}
\operatorname{Re} w\left(e^{i\frac{\pi}{a}(\xi+x)}e^{-\frac{\pi}{a}(b-y+\eta)}, \frac{\pi b}{a}\right) &= -2\operatorname{Re}\left(\log\prod_{k=0}^{\infty}\left(1-e^{i\frac{\pi}{a}(\xi+x)}e^{-\frac{\pi}{a}(b-y+\eta)}e^{-\frac{\pi b}{a}}\left(e^{-\frac{2\pi b}{a}}\right)^k\right)\right)\\
&= -2\operatorname{Re}\left(\log\prod_{k=0}^{\infty}\left(1-e^{i\frac{\pi}{a}(\xi+x)}e^{\frac{\pi}{a}(y-\eta)}\left(e^{-\frac{2\pi b}{a}}\right)^{k+1}\right)\right)\\
&= -2\log\prod_{k=1}^{\infty}\left|1-e^{i\frac{\pi}{a}(\xi+x)}e^{\frac{\pi}{a}(y-\eta)}\left(e^{-\frac{2\pi b}{a}}\right)^k\right|
\end{aligned}$$

and

$$\begin{aligned}
\left|1-e^{i\frac{\pi}{a}(\xi+x)}e^{\frac{\pi}{a}(y-\eta)}\left(e^{-\frac{2\pi b}{a}}\right)^k\right| &= \left|1-e^{i\frac{\pi}{a}(\xi+x)}e^{\frac{\pi}{a}(y-\eta)}q^k\right|\\
&= \left|1-\cos\left(\frac{\pi}{a}(\xi+x)\right)e^{\frac{\pi}{a}(y-\eta)}q^k - i\sin\left(\frac{\pi}{a}(\xi+x)\right)e^{\frac{\pi}{a}(y-\eta)}q^k\right|\\
&= \sqrt{\left(1-\cos\left(\frac{\pi}{a}(\xi+x)\right)e^{\frac{\pi}{a}(y-\eta)}q^k\right)^2 + \left(\sin\left(\frac{\pi}{a}(\xi+x)\right)e^{\frac{\pi}{a}(y-\eta)}q^k\right)^2}\\
&= \sqrt{1-2\cos\left(\frac{\pi}{a}(\xi+x)\right)e^{\frac{\pi}{a}(y-\eta)}q^k + e^{2\frac{\pi}{a}(y-\eta)}q^{2k}}
\end{aligned}$$

Thus,

$$\operatorname{Re} w\left(e^{i\frac{\pi}{a}(\xi+x)}e^{-\frac{\pi}{a}(b-y+\eta)}, \frac{\pi b}{a}\right) = -\log\prod_{k=1}^{\infty}\left(1-2\cos\left(\frac{\pi}{a}(\xi+x)\right)e^{\frac{\pi}{a}(y-\eta)}q^k + e^{2\frac{\pi}{a}(y-\eta)}q^{2k}\right)$$

On the other hand,

$$\begin{aligned}
\operatorname{Re} w\left(e^{i\frac{\pi}{a}(\xi+x)}e^{\frac{\pi}{a}(b-y+\eta)}, \frac{\pi b}{a}\right) &= -2\operatorname{Re}\left(\log\prod_{k=0}^{\infty}\left(1-e^{i\frac{\pi}{a}(\xi+x)}e^{\frac{\pi}{a}(b-y+\eta)}e^{-\frac{\pi b}{a}}\left(e^{-\frac{2\pi b}{a}}\right)^k\right)\right)\\
&= -2\operatorname{Re}\left(\log\prod_{k=0}^{\infty}\left(1-e^{i\frac{\pi}{a}(\xi+x)}e^{-\frac{\pi}{a}(y-\eta)}\left(e^{-\frac{2\pi b}{a}}\right)^k\right)\right)\\
&= -2\log\prod_{k=0}^{\infty}\left|1-e^{i\frac{\pi}{a}(\xi+x)}e^{-\frac{\pi}{a}(y-\eta)}\left(e^{-\frac{2\pi b}{a}}\right)^k\right|
\end{aligned}$$

is

$$\operatorname{Re} w\left(e^{i\frac{\pi}{a}(\xi+x)}e^{\frac{\pi}{a}(b-y+\eta)}, \frac{\pi b}{a}\right) = -\log\prod_{k=0}^{\infty}\left(1-2\cos\left(\frac{\pi}{a}(\xi+x)\right)e^{-\frac{\pi}{a}(y-\eta)}q^k + e^{-2\frac{\pi}{a}(y-\eta)}q^{2k}\right)$$

Hence,

$$\begin{aligned}
T_q(x,y;\xi,\eta) &= \frac{\operatorname{Re}\left\{w\left(e^{i\frac{\pi}{a}(\xi+x)}e^{-\frac{\pi}{a}(b-y+\eta)}, \frac{\pi b}{a}\right) + w\left(e^{i\frac{\pi}{a}(\xi+x)}e^{\frac{\pi}{a}(b-y+\eta)}, \frac{\pi b}{a}\right)\right\}}{4\pi}\\
&= -\frac{1}{4\pi}\log\prod_{k=1}^{\infty}\left(1-2\cos\left(\frac{\pi}{a}(\xi+x)\right)e^{\frac{\pi}{a}(y-\eta)}q^k + e^{2\frac{\pi}{a}(y-\eta)}q^{2k}\right)\\
&\quad -\frac{1}{4\pi}\log\prod_{k=0}^{\infty}\left(1-2\cos\left(\frac{\pi}{a}(\xi+x)\right)e^{-\frac{\pi}{a}(y-\eta)}q^k + e^{-2\frac{\pi}{a}(y-\eta)}q^{2k}\right)
\end{aligned}$$

which leads to (25). The argument of the log in the first term of (25) is

$$\begin{aligned}1-2\cos\left(\frac{\pi}{a}\left(\xi\pm x\right)\right)e^{-\frac{\pi}{a}(y-\eta)}+e^{-2\frac{\pi}{a}(y-\eta)} &= 1-2e^{-\frac{\pi}{a}(y-\eta)}\left(1-2\sin^2\left(\frac{\pi}{2a}\left(\xi\pm x\right)\right)\right)+e^{-2\frac{\pi}{a}(y-\eta)}\\ &= 1-2e^{-\frac{\pi}{a}(y-\eta)}+4e^{-\frac{\pi}{a}(y-\eta)}\sin^2\left(\frac{\pi}{2a}\left(\xi\pm x\right)\right)+e^{-2\frac{\pi}{a}(y-\eta)}\\ &= \left(1-e^{-\frac{\pi}{a}(y-\eta)}\right)^2+\left(2e^{-\frac{\pi}{2a}(y-\eta)}\sin\left(\frac{\pi}{2a}\left(\xi\pm x\right)\right)\right)^2\end{aligned}$$

which more clearly indicates that $e^{-\frac{\pi}{a}(y-\eta)}\leq 1$ in the interval $0\leq\eta\leq y$ and only equal to 1 if $y=\eta$.

D.2 Current density

In the interval $0\leq\eta\leq y$, the partial derivative of the single sum quasi-Green's function (22) is

$$\frac{\partial K\left(x,y,\xi,\eta\right)}{\partial x}=\frac{2}{a}\sum_{n=1}^{\infty}\frac{\cosh\frac{\pi n}{a}\left(b-y\right)\cosh\frac{\pi n}{a}\eta}{\sinh\left(\frac{\pi n}{a}b\right)}\cos\left(\frac{\pi n}{a}\xi\right)\sin\left(\frac{\pi n}{a}x\right)$$

We repeat the method of Section D.1. After invoking $2\sin a\cos b=\sin\left(a+b\right)+\sin\left(a-b\right)$, the n-sum is

$$\begin{aligned}S'=&\frac{1}{a}\sum_{n=1}^{\infty}\frac{\cosh\frac{\pi n}{a}\left(b-y\right)\cosh\frac{\pi n}{a}\eta}{\sinh\left(\frac{\pi n}{a}b\right)}\sin\left(\frac{\pi n}{a}\left(\xi+x\right)\right)\\ &+\frac{1}{a}\sum_{n=1}^{\infty}\frac{\cosh\frac{\pi n}{a}\left(b-y\right)\cosh\frac{\pi n}{a}\eta}{\sinh\left(\frac{\pi n}{a}b\right)}\sin\left(\frac{\pi n}{a}\left(\xi-x\right)\right)\end{aligned}$$

Similarly, with $2\cosh a\cosh b=\cosh\left(a+b\right)+\cosh\left(a-b\right)$, we have that

$$\begin{aligned}S'=&\frac{1}{2a}\sum_{n=1}^{\infty}\frac{\cosh\frac{\pi n}{a}\left(b-y+\eta\right)}{\sinh\left(\frac{\pi n}{a}b\right)}\sin\left(\frac{\pi n}{a}\left(\xi+x\right)\right)+\\ &+\frac{1}{2a}\sum_{n=1}^{\infty}\frac{\cosh\frac{\pi n}{a}\left(b-y-\eta\right)}{n\sinh\left(\frac{\pi n}{a}b\right)}\sin\left(\frac{\pi n}{a}\left(\xi+x\right)\right)\\ &+\frac{1}{2a}\sum_{n=1}^{\infty}\frac{\cosh\frac{\pi n}{a}\left(b-y+\eta\right)}{\sinh\left(\frac{\pi n}{a}b\right)}\sin\left(\frac{\pi n}{a}\left(\xi-x\right)\right)\\ &+\frac{1}{2a}\sum_{n=1}^{\infty}\frac{\cosh\frac{\pi n}{a}\left(b-y-\eta\right)}{\sinh\left(\frac{\pi n}{a}b\right)}\sin\left(\frac{\pi n}{a}\left(\xi-x\right)\right)\end{aligned}$$

Finally, with $\cosh a=\cos ia$ and again $2\sin a\cos b=\sin\left(a+b\right)+\sin\left(a-b\right)$, we find the reduction

$$\begin{aligned}S=&\frac{1}{4a}\sum_{n=1}^{\infty}\frac{\sin\frac{\pi n}{a}\left(\left(\xi+x\right)+i\left(b-y+\eta\right)\right)}{\sinh\left(\frac{\pi n}{a}b\right)}+\frac{1}{4a}\sum_{n=1}^{\infty}\frac{\sin\frac{\pi n}{a}\left(\left(\xi+x\right)-i\left(b-y+\eta\right)\right)}{\sinh\left(\frac{\pi n}{a}b\right)}\\ &+\frac{1}{4a}\sum_{n=1}^{\infty}\frac{\sin\frac{\pi n}{a}\left(\left(\xi+x\right)+i\left(b-y-\eta\right)\right)}{\sinh\left(\frac{\pi n}{a}b\right)}+\frac{1}{4a}\sum_{n=1}^{\infty}\frac{\sin\frac{\pi n}{a}\left(\left(\xi+x\right)-i\left(b-y-\eta\right)\right)}{\sinh\left(\frac{\pi n}{a}b\right)}\\ &+\frac{1}{4a}\sum_{n=1}^{\infty}\frac{\sin\frac{\pi n}{a}\left(\left(\xi-x\right)+i\left(b-y+\eta\right)\right)}{\sinh\left(\frac{\pi n}{a}b\right)}+\frac{1}{4a}\sum_{n=1}^{\infty}\frac{\sin\frac{\pi n}{a}\left(\left(\xi-x\right)-i\left(b-y+\eta\right)\right)}{\sinh\left(\frac{\pi n}{a}b\right)}\\ &+\frac{1}{4a}\sum_{n=1}^{\infty}\frac{\sin\frac{\pi n}{a}\left(\left(\xi-x\right)+i\left(b-y-\eta\right)\right)}{\sinh\left(\frac{\pi n}{a}b\right)}+\frac{1}{4a}\sum_{n=1}^{\infty}\frac{\sin\frac{\pi n}{a}\left(\left(\xi-x\right)-i\left(b-y-\eta\right)\right)}{\sinh\left(\frac{\pi n}{a}b\right)}\end{aligned}$$

With $\sin x = \frac{e^{ix}-e^{-ix}}{2i} = \mathrm{Im}\left(e^{ix}\right)$, $A = \frac{\pi b}{a}$ and the definition (37) of the function $w(z,A) = \sum_{n=1}^{\infty} \frac{z^n}{n\sinh(An)}$, each of the sums is of the type

$$z\frac{\partial w(z,A)}{\partial z} = \sum_{n=1}^{\infty} \frac{z^n}{\sinh(An)}$$

which also equals, after derivation of (49),

$$W(z,A) = z\frac{\partial w(z,A)}{\partial z} = zw'(z,A) = 2\sum_{k=0}^{\infty} \frac{ze^{-A}q^k}{1-ze^{-A}q^k} = 2\sum_{k=0}^{\infty} \frac{z}{e^{A(1+2k)}-z} \tag{38}$$

Thus, the partial x-derivative of single sum quasi-Green's function (22) in the interval $0 \le \eta \le y$ is

$$\begin{aligned}\frac{\partial K(x,y,\xi,\eta)}{\partial x} = &\frac{\mathrm{Im}\left\{W\left(e^{i\frac{\pi}{a}(\xi+x)}e^{-\frac{\pi}{a}(b-y+\eta)}, \frac{\pi b}{a}\right) + W\left(e^{i\frac{\pi}{a}(\xi+x)}e^{\frac{\pi}{a}(b-y+\eta)}, \frac{\pi b}{a}\right)\right\}}{4a} \\ &+ \frac{\mathrm{Im}\left\{W\left(e^{i\frac{\pi}{a}(\xi+x)}e^{-\frac{\pi}{a}(b-y-\eta)}, \frac{\pi b}{a}\right) + W\left(e^{i\frac{\pi}{a}(\xi+x)}e^{\frac{\pi}{a}(b-y-\eta)}, \frac{\pi b}{a}\right)\right\}}{4a} \\ &+ \frac{\mathrm{Im}\left\{W\left(e^{i\frac{\pi}{a}(\xi-x)}e^{-\frac{\pi}{a}(b-y+\eta)}, \frac{\pi b}{a}\right) + W\left(e^{i\frac{\pi}{a}(\xi-x)}e^{\frac{\pi}{a}(b-y+\eta)}, \frac{\pi b}{a}\right)\right\}}{4a} \\ &+ \frac{\mathrm{Im}\left\{W\left(e^{i\frac{\pi}{a}(\xi-x)}e^{-\frac{\pi}{a}(b-y-\eta)}, \frac{\pi b}{a}\right) + W\left(e^{i\frac{\pi}{a}(\xi-x)}e^{\frac{\pi}{a}(b-y-\eta)}, \frac{\pi b}{a}\right)\right\}}{4a}\end{aligned} \tag{39}$$

For complex $z = X + iY$, it holds that

$$w'(X+iY,A) = 2\sum_{k=0}^{\infty} \frac{1}{e^{A(1+2k)}-X-iY} = 2\sum_{k=0}^{\infty} \frac{e^{A(1+2k)}-X+iY}{\left(e^{A(1+2k)}-X\right)^2+Y^2}$$

and

$$\begin{aligned}W(X+iY,A) &= (X+iY)\,w'(X+iY,A) = 2\sum_{k=0}^{\infty} \frac{\left(\left(e^{A(1+2k)}-X\right)+iY\right)(X+iY)}{\left(e^{A(1+2k)}-X\right)^2+Y^2} \\ &= 2\sum_{k=0}^{\infty} \frac{e^{A(1+2k)}-\left(X^2+Y^2\right)+iYe^{A(1+2k)}}{\left(e^{A(1+2k)}-X\right)^2+Y^2}\end{aligned}$$

from which it follows that

$$\mathrm{Im}\left(W(X+iY,A)\right) = 2\sum_{k=0}^{\infty} \frac{Ye^{A(1+2k)}}{\left(e^{A(1+2k)}-X\right)^2+Y^2}$$

allowing the computation of $\frac{\partial K(x,y,\xi,\eta)}{\partial x}$ in (39).

Since the rectangle can be considered as the fundamental parallelogram P, whose repetition covers the entire complex plane, the real functions $h_{\mathrm{Re}}(x,y) = \frac{\partial K(x,y,x_{in},y_{in})}{\partial x} - \frac{\partial K(x,y,x_{out},y_{out})}{\partial x}$ and $h_{\mathrm{Im}}(x,y) = \frac{\partial K(x,y,x_{in},y_{in})}{\partial y} - \frac{\partial K(x,y,x_{out},y_{out})}{\partial y}$ are the real and imaginary part of a complex function $h(z)$ in the complex number $z = x + iy$,

$$h(z) = h(x+iy) = h_{\mathrm{Re}}(x,y) + ih_{\mathrm{Im}}(x,y)$$

that is zero on the boundaries of the rectangle. Analytic functions achieve their extrema at the boundary. The complex function $h(z)$ is thus double-periodic in the complex complex plane and is an

elliptic function [17, Chapter I & II]. Indeed, $h(z)$ is not an entire function, for it would be bounded in the rectangle and due to periodicity, $h(z)$ would be bounded over the entire complex plane in which case Liouville's theorem then indicates that $h(z)$ is a constant. Second, $h(z)$ must have an even number of poles and zeros in the rectangle, because $\int_P h(z)\,dz = 0$. The derivative of an elliptic function is also elliptic, but its integral is not necessarily an elliptic function [17].

E The effective resistance in the continuum RGG

The corresponding resistance of the 3D beam, due to current injection at point $s = (x_{in}, y_{in}, 0)$ and ejection at point $d = (x_{out}, y_{out}, 0)$ follows from the law of Ohm with the voltage (10) as

$$\begin{aligned} R_{sd} &= \frac{V(x_{in}, y_{in}, 0) - V(x_{out}, y_{out}, 0)}{I} \\ &= \frac{4\varrho}{ab} \sum_{k=0}^{\infty} \sum_{l=0}^{\infty} \gamma_{kl} \frac{\left(\cos\frac{k\pi}{a} x_{in} \cos\frac{l\pi}{b} y_{in} - \cos\frac{k\pi}{a} x_{out} \cos\frac{l\pi}{b} y_{out}\right)^2}{\sqrt{\left(\frac{k\pi}{a}\right)^2 + \left(\frac{l\pi}{b}\right)^2}} \coth\left(c\sqrt{\left(\frac{k\pi}{a}\right)^2 + \left(\frac{l\pi}{b}\right)^2}\right) \end{aligned} \tag{40}$$

where $\gamma_{00} = 0, \gamma_{k0} = \gamma_{0l} = \frac{1}{2}$ and $\gamma_{kl} = 1$ for $k > 0$ and $l > 0$; a notation that is also used in (31). The last relation shows that the resistance is always non-negative, i.e. $R_{sd} \geq 0$.

The resistance R_{sd} is the proportionality constant that connects the voltage difference between the injection point s and the ejection point d and the current I in the physical 3D world, due to Ohm's law. Choosing a unit current of 1 Ampere with its associated voltage difference simplifies the above definition of the "effective" resistance between point s and d to $\omega_{sd} = R_{sd}|_{I=1\text{ Ampere}}$. In particular in the limit towards 2D, which is not physical[11], but a mathematical generalization, we are led to define the "effective" resistance between node s and node d in the continuum RGG as

$$\omega_{sd} = V(x_{in}, y_{in}) - V(x_{out}, y_{out}) \tag{41}$$

The definition (41) circumvents difficulties due the renormalization $\frac{\varrho I}{c} = 1$ in Section 4.1. Thus, similarly as in Section 4.1, we find, either from the 3D resistance (40) with the renormalization $\frac{\varrho I}{c} = 1$ or from (41) and (12), the double Fourier series for "effective" resistance between node s and node d in the continuum RGG

$$\begin{aligned} \omega_{sd} = \frac{2}{ab} \lim_{K\to\infty} \sum_{k=1}^{K} \frac{\left(\cos\frac{k\pi}{a} x_{in} - \cos\frac{k\pi}{a} x_{out}\right)^2}{\left(\frac{k\pi}{a}\right)^2} + \frac{2}{ab} \sum_{l=1}^{K} \frac{\left(\cos\frac{l\pi}{b} y_{in} - \cos\frac{l\pi}{b} y_{out}\right)^2}{\left(\frac{l\pi}{b}\right)^2} \\ + \frac{4}{ab} \sum_{k=1}^{K} \sum_{l=1}^{K} \frac{\left(\cos\frac{k\pi}{a} x_{in} \cos\frac{l\pi}{b} y_{in} - \cos\frac{k\pi}{a} x_{out} \cos\frac{l\pi}{b} y_{out}\right)^2}{\left(\frac{k\pi}{a}\right)^2 + \left(\frac{l\pi}{b}\right)^2} \end{aligned} \tag{42}$$

E.1 The effective resistance ω_{sd} in (42) does not exist

The single sums in (42) converge (and can be written in terms of the polylogarithm function $\mathrm{Li}_k(z) = \sum_{n=1}^{\infty} \frac{z^n}{n^k}$), but we will demonstrate here that the double sum S in (42) diverges.

Indeed, all the terms are non-negative. Moreover, only a finite number of terms are zero, i.e.

$$t_{kl} = \cos\frac{k\pi}{a} x_{in} \cos\frac{l\pi}{b} y_{in} - \cos\frac{k\pi}{a} x_{out} \cos\frac{l\pi}{b} y_{out} = 0$$

[11] Although electrons are tiny, they live in 3D and do not exist in 2D.

which happens, for $m_j \in \mathbb{Z}$ for $j = 1, 2, 3, 4$, if

$$\begin{aligned}
&\left\{\left\{k\frac{x_{in}}{a} = \frac{1}{2} + m_1\right\} \cap \left\{k\frac{x_{out}}{a} = \frac{1}{2} + m_2\right\}\right\} \\
&\cup \left\{\left\{k\frac{x_{in}}{a} = \frac{1}{2} + m_1\right\} \cap \left\{l\frac{y_{out}}{b} = \frac{1}{2} + m_3\right\}\right\} \\
&\cup \left\{\left\{l\frac{y_{in}}{b} = \frac{1}{2} + m_4\right\} \cap \left\{k\frac{x_{out}}{a} = \frac{1}{2} + m_2\right\}\right\} \\
&\cup \left\{\left\{l\frac{y_{in}}{b} = \frac{1}{2} + m_4\right\} \cap \left\{l\frac{y_{out}}{b} = \frac{1}{2} + m_3\right\}\right\}
\end{aligned}$$

Now, $k\frac{2x_{in}}{a} = 1 + m_1$ requires that $\frac{2x_{in}}{a} = \frac{n_1}{n_2} \in \mathbb{Q}$, where both n_1 and n_2 are non-negative integers, because $0 \leq x_{in} \leq a$. If $\frac{x_{in}}{a}$, $\frac{x_{out}}{a}$, $\frac{y_{in}}{b}$ and $\frac{y_{out}}{b}$ are not rational numbers (that form the overwhelming majority of cases), then there does not exist any pair (k, l) of positive integers for which any term t_{kl} is zero. Hence, there exist a positive number

$$\beta = \frac{4}{ab} \min_{(k,l)} \left(\cos\frac{k\pi}{a}x_{in}\ \cos\frac{l\pi}{b}y_{in} - \cos\frac{k\pi}{a}x_{out}\ \cos\frac{l\pi}{b}y_{out}\right)^2$$

so that double sum S in (42) is lower bounded by

$$S > \beta \sum_{k=1}^{\infty}\sum_{l=1}^{\infty} \frac{1}{\left(\frac{k\pi}{a}\right)^2 + \left(\frac{l\pi}{b}\right)^2} = \beta H(a, b) \tag{43}$$

The complex number $\frac{k\pi}{a} + i\frac{l\pi}{b}$ has the square norm $\left|\frac{k\pi}{a} + i\frac{l\pi}{b}\right|^2 = \left(\frac{k\pi}{a}\right)^2 + \left(\frac{l\pi}{b}\right)^2$. We now review some basics from elliptic function theory and follow Rademacher [18, Chapter 8]. Let ω_1 and ω_2 be two complex numbers, different from zero, such that their quotient $\tau = \frac{\omega_2}{\omega_1}$ is not real. The totality Ω of all complex numbers $m_1\omega_1 + m_2\omega_2$, with integers m_1 and m_2, forms a point-lattice in the complex plane. The Eisenstein series

$$G_p(\omega_1, \omega_2) = \sum_{(m_1,m_2)\neq(0,0)} \frac{1}{(m_1\omega_1 + m_2\omega_2)^p} \tag{44}$$

sums over all pairs (m_1, m_2) of integers, except for the pair $m_1 = m_2 = 0$. Rademacher [18, Lemma, p. 117] proofs Eisenstein's convergence lemma that, for $p > 2$, the series

$$\sum_{(m_1,m_2)\neq(0,0)} \frac{1}{|m_1\omega_1 + m_2\omega_2|^p}$$

is convergent. We return to our series $H(a, b)$, which satisfies

$$\left|\sum_{k=1}^{\infty}\sum_{l=1}^{\infty} \frac{1}{\left(\frac{k\pi}{a} + i\frac{l\pi}{b}\right)^2}\right| \leq \sum_{k=1}^{\infty}\sum_{l=1}^{\infty} \frac{1}{\left(\frac{k\pi}{a}\right)^2 + \left(\frac{l\pi}{b}\right)^2}$$

The left-hand side is a special case of an Eisenstein series (44) with $\omega_1 = \frac{\pi}{a}$ and $\omega_2 = i\frac{\pi}{b}$, which does not converge absolutely, because $p = 2$, whereas convergence demands a strictly larger value of p than

2. A convergent series with exponent $p = 2$ has led Weierstrass[12] to propose his famous, basic elliptic function

$$\wp(u) = \frac{1}{u^2} + \sum_{(m_1,m_2)\neq(0,0)} \left(\frac{1}{(u-(m_1\omega_1+m_2\omega_2))^2} - \frac{1}{(m_1\omega_1+m_2\omega_2)^2} \right) \tag{45}$$

In summary, we arrive at the conclusion that the double sum $H(a,b) \to \infty$ and that the effective resistance ω_{sd} in (42) does not exist. An alternative proof of the non-existence of the effective resistance ω_{sd}, based on our q-series, is given in Appendix E.2.

Due to the fact that $p = 2$ in double sum $H(a,b)$ in (43), whereas Eisenstein's convergence lemma requires $p = 2+\varepsilon$, with $\varepsilon > 0$ but arbitrarily small, numerical evaluations of the double Fourier series ω_{sd} in (42) diverge extremely slowly. For example, for a source node $s = (1/8, 3/8)$ and a drain node $d = (3/4, 3/4)$, the effective resistance $\omega_{sd}(K)$ increase with the number terms K as $\omega_{sd}(1000) = 2.79642$, $\omega_{sd}(2000) = 3.0169$, $\omega_{sd}(3000) = 3.14591 \approx \pi$, $\omega_{sd}(4000) = 3.23745$, $\omega_{sd}(5000) = 3.30846$ and $\omega_{sd}(10^4) = 3.52907$.

E.2 Alternative demonstration of non-existence of the effective resistance ω_{sd} in (42)

The "effective" resistance (41) in 2D between node $s = (x_{in}, y_{in})$ and node $d = (x_{out}, y_{out})$ becomes with the Green's function $V(x,y) = K(x,y;x_{in},y_{in}) - K(x,y;x_{out},y_{out})$ in (13)

$$\omega_{sd} = K(x_{in},y_{in};x_{in},y_{in}) - K(x_{in},y_{in};x_{out},y_{out}) - K(x_{out},y_{out};x_{in},y_{in}) + K(x_{out},y_{out};x_{out},y_{out}) \tag{46}$$

Invoking the q-extension (24)

$$K(x,y,\xi,\eta) = \frac{1}{a} g_0(y,\eta) + T_q(x,y;\xi,\eta) + T_q(x,y;\xi,-\eta) + T_q(-x,y;\xi,\eta) + T_q(-x,y;\xi,-\eta)$$

then yields

$$K(\xi,\eta,\xi,\eta) = T_q(\xi,\eta;\xi,\eta) + T_q(-\xi,\eta;\xi,\eta) + T_q(\xi,\eta;\xi,-\eta) + T_q(-\xi,\eta;\xi,-\eta)$$

The definition (25) of $T_q(x,y;\xi,\eta)$

$$\begin{aligned} T_q(x,y;\xi,\eta) = &-\frac{1}{4\pi}\log\left(1-2\cos\left(\frac{\pi}{a}(\xi+x)\right)e^{-\frac{\pi}{a}(y-\eta)} + e^{-2\frac{\pi}{a}(y-\eta)}\right) \\ &-\frac{1}{4\pi}\log\prod_{k=1}^{\infty}\left(1-2\cos\left(\frac{\pi}{a}(\xi+x)\right)e^{\frac{\pi}{a}(y-\eta)}q^k + e^{2\frac{\pi}{a}(y-\eta)}q^{2k}\right) \\ &\times\left(1-2\cos\left(\frac{\pi}{a}(\xi+x)\right)e^{-\frac{\pi}{a}(y-\eta)}q^k + e^{-2\frac{\pi}{a}(y-\eta)}q^{2k}\right) \end{aligned}$$

simplifies for $y = \eta$ to

$$T_q(x,\eta;\xi,\eta) = -\frac{1}{2\pi}\log\left(2\sin\left(\frac{\pi}{2a}(\xi+x)\right)\right) - \frac{1}{2\pi}\log\prod_{k=1}^{\infty}\left(1-2\cos\left(\frac{\pi}{a}(\xi+x)\right)q^k + q^{2k}\right)$$

[12] Weierstrass's $\wp(u)$ function can be regarded as a generalization to a two-dimensions complex lattice of Gauss's digamma function $\psi(u) = \frac{d}{du}\log\Gamma(u)$ in [10, Chapter 12], because

$$\psi(u+1) = -\gamma - \sum_{n=1}^{\infty}\left(\frac{1}{u+n} - \frac{1}{n}\right)$$

Further, we find that

$$T_q(\xi,\eta;\xi,\eta) = -\frac{1}{2\pi}\log\left(2\left|\sin\left(\frac{\pi}{a}\xi\right)\right|\right) - \frac{1}{2\pi}\log\prod_{k=1}^{\infty}\left(1+q^{2k}-2q^k\cos\left(\frac{2\pi}{a}\xi\right)\right)$$

and that

$$\lim_{x\to-\xi} T_q(x,\eta;\xi,\eta) = -\frac{1}{2\pi}\lim_{x\to-\xi}\log\left(2\sin\left(\frac{\pi}{2a}(\xi+x)\right)\right) - \frac{1}{\pi}\log\prod_{k=1}^{\infty}\left(1-q^k\right)$$

Similarly, the definition (25) of $T_q(x,y;\xi,\eta)$ indicates that

$$\begin{aligned} T_q(x,\eta;\xi,-\eta) = &-\frac{1}{4\pi}\log\left(1-2\cos\left(\frac{\pi}{a}(\xi+x)\right)e^{-\frac{2\pi}{a}\eta}+e^{-\frac{4\pi}{a}\eta}\right) \\ &-\frac{1}{4\pi}\log\prod_{k=1}^{\infty}\left(1-2\cos\left(\frac{\pi}{a}(\xi+x)\right)e^{\frac{2\pi}{a}\eta}q^k+e^{\frac{4\pi}{a}\eta}q^{2k}\right) \\ &\times\left(1-2\cos\left(\frac{\pi}{a}(\xi+x)\right)e^{-\frac{2\pi}{a}\eta}q^k+e^{-\frac{4\pi}{a}\eta}q^{2k}\right) \end{aligned}$$

from which

$$\begin{aligned} T_q(\xi,\eta;\xi,-\eta) = &-\frac{1}{4\pi}\log\left(1-2\cos\left(\frac{2\pi}{a}\xi\right)e^{-\frac{2\pi}{a}\eta}+e^{-\frac{4\pi}{a}\eta}\right) \\ &-\frac{1}{4\pi}\log\prod_{k=1}^{\infty}\left(1-2\cos\left(\frac{2\pi}{a}\xi\right)e^{\frac{2\pi}{a}\eta}q^k+e^{\frac{4\pi}{a}\eta}q^{2k}\right)\left(1-2\cos\left(\frac{2\pi}{a}\xi\right)e^{-\frac{2\pi}{a}\eta}q^k+e^{-\frac{4\pi}{a}\eta}q^{2k}\right) \end{aligned}$$

and

$$\begin{aligned} T_q(-\xi,\eta;\xi,-\eta) = &-\frac{1}{2\pi}\log\left(1-e^{-\frac{2\pi}{a}\eta}\right) \\ &-\frac{1}{4\pi}\log\prod_{k=1}^{\infty}\left(1-2e^{\frac{2\pi}{a}\eta}q^k+e^{\frac{4\pi}{a}\eta}q^{2k}\right)\left(1-2e^{-\frac{2\pi}{a}\eta}q^k+e^{-\frac{4\pi}{a}\eta}q^{2k}\right) \end{aligned}$$

Hence, we observe that only in the term $\lim_{x\to-\xi} T_q(x,\eta;\xi,\eta)$, a logarithmic divergence occurs of the type $-\frac{1}{2\pi}\lim_{x\to-\xi}\log\left(2\sin\left(\frac{\pi}{2a}(\xi+x)\right)\right)$. Such a term occurs both in $K(x_{in},y_{in};x_{in},y_{in})$ and $K(x_{out},y_{out};x_{out},y_{out})$ with the same sign. Since the remaining contributions $K(x_{in},y_{in};x_{out},y_{out}) + K(x_{out},y_{out};x_{in},y_{in})$ do not contain a divergent term, we again find that the effective resistance ω_{sd} in (46) does not exist.

E.3 The resistance R_{sd} in (40) in 3D does not exist either

Since $\coth\left(c\sqrt{\left(\frac{k\pi}{a}\right)^2+\left(\frac{l\pi}{b}\right)^2}\right)$ rapidly tends to 1 for sufficiently large k and l in the 3D resistance (40) the corresponding double sum tends to

$$S_{3D} \simeq \frac{4\varrho}{ab}\sum_{k=K_k}^{\infty}\sum_{l=K_k}^{\infty}\frac{\left(\cos\frac{k\pi}{a}x_{in}\cos\frac{l\pi}{b}y_{in}-\cos\frac{k\pi}{a}x_{out}\cos\frac{l\pi}{b}y_{out}\right)^2}{\sqrt{\left(\frac{k\pi}{a}\right)^2+\left(\frac{l\pi}{b}\right)^2}}$$

By a similar argument as Section E.1 and Eisenstein's convergence lemma, we conclude that also the resistance R_{sd} in (40) in 3D does not exist!

E.4 Consequence for the effective resistance ω_{sd} in RGG

Although our mathematical derivations are correct, the computation of a simple physical concept as the resistance reveals an error. The error is a "modeling fault" of reality: the assumption of current in- and ejection in a point relies on delta functions that simplify the mathematical equations. However, forcing a current to pass through a single point with zero dimensions causes the resistance between injection point s and ejection point d to grow infinitely large, for any configuration of the pair (s,d).

We replace the point injection by a small finite area. The simplest form in our Euclidian coordinate frame is a rectangular in- and ejection area over which the current is homogeneously spread with constant the current density $j = \frac{I}{h_{xin}h_{yin}}$, which results in the function $g(x,y)$ in Section 3.4,

$$g(x,y) = \begin{cases} \frac{\varrho I}{h_{xin}h_{yin}} \text{ for } x_{in} - \frac{h_{xin}}{2} \leq x \leq x_{in} + \frac{h_{xin}}{2} \text{ and } y_{in} - \frac{h_{yin}}{2} \leq y \leq y_{in} + \frac{h_{yin}}{2} \\ \frac{\varrho I}{h_{xout}h_{yout}} \text{ for } x_{out} - \frac{h_{xout}}{2} \leq x \leq x_{out} + \frac{h_{xout}}{2} \text{ and } y_{out} - \frac{h_{yout}}{2} \leq x \leq y_{out} + \frac{h_{yout}}{2} \end{cases}$$

The correspondingly modified Fourier coefficients follow from (9) and require the computations of the double integral

$$\begin{aligned} I_2 &= \int_0^a dx \int_0^b dy\, g(x,y) \cos\frac{k\pi x}{a} \cos\frac{l\pi y}{b} = \frac{\varrho I}{h_{xin}h_{yin}} \int_{x_{in}-\frac{h_{xin}}{2}}^{x_{in}+\frac{h_{xin}}{2}} \cos\frac{k\pi x}{a} dx \int_{y_{in}-\frac{h_{yin}}{2}}^{y_{in}+\frac{h_{yin}}{2}} \cos\frac{l\pi y}{b} dy \\ &= \frac{\varrho I}{h_{xin}h_{yin}} \frac{\sin\frac{k\pi}{a}\left(x_{in}+\frac{h_{xin}}{2}\right) - \sin\frac{k\pi}{a}\left(x_{in}-\frac{h_{xin}}{2}\right)}{\frac{k\pi}{a}} \frac{\sin\frac{l\pi}{b}\left(y_{in}+\frac{h_{xin}}{2}\right) - \sin\frac{l\pi}{b}\left(x_{in}-\frac{h_{xin}}{2}\right)}{\frac{l\pi}{b}} \\ &= \varrho I \cos\left(\frac{k\pi}{a}x_{in}\right) \cos\left(\frac{l\pi}{b}y_{in}\right) \times \frac{\sin\left(\frac{k\pi}{a}\frac{h_{xin}}{2}\right)}{\frac{k\pi}{a}\frac{h_{xin}}{2}} \frac{\sin\left(\frac{l\pi}{b}\frac{h_{yin}}{2}\right)}{\frac{l\pi}{b}\frac{h_{yin}}{2}} \end{aligned}$$

Comparing the point injection in Section 3.4 with a non-zero rectangular area injection reveals that only a product of $\mathrm{sinc}(X) = \frac{\sin X}{X}$ is added. Provided that the rectangular injection area completely lies within the xy-face of the beam, i.e. $\left\{0 \leq x_{in} - \frac{h_{xin}}{2}\right\} \cap \left\{x_{in} + \frac{h_{xin}}{2} \leq a\right\}$ and $\left\{0 \leq y_{in} - \frac{h_{yin}}{2}\right\} \cap \left\{y_{in} + \frac{h_{yin}}{2} \leq b\right\}$ and similarly for the rectangular ejection area, the modified 3D voltage is, corresponding to (10), is

$$\begin{aligned} V(x,y,z) + V_{\mathrm{ref}} = {} & \frac{2\varrho I}{ab} \sum_{k=1}^{\infty} \frac{\left(\cos\frac{k\pi}{a}x_{in} \frac{\sin\left(\frac{k\pi}{a}\frac{h_{xin}}{2}\right)}{\frac{k\pi}{a}\frac{h_{xin}}{2}} - \cos\frac{k\pi}{a}x_{out} \frac{\sin\left(\frac{k\pi}{a}\frac{h_{xout}}{2}\right)}{\frac{k\pi}{a}\frac{h_{xout}}{2}}\right)}{\frac{k\pi}{a}\sinh\left(c\frac{k\pi}{a}\right)} \cos\frac{k\pi}{a}x \cosh\left(\frac{k\pi}{a}(z-c)\right) \\ & + \frac{2\varrho I}{ab} \sum_{l=1}^{\infty} \frac{\left(\cos\frac{l\pi}{b}y_{in} \frac{\sin\left(\frac{l\pi}{b}\frac{h_{yin}}{2}\right)}{\frac{l\pi}{b}\frac{h_{yin}}{2}} - \cos\frac{l\pi}{b}y_{out} \frac{\sin\left(\frac{l\pi}{b}\frac{h_{yout}}{2}\right)}{\frac{l\pi}{b}\frac{h_{yout}}{2}}\right)}{\frac{l\pi}{b}\sinh\left(c\frac{l\pi}{b}\right)} \cos\frac{l\pi}{b}y \cosh\left(\frac{l\pi}{b}(z-c)\right) \\ & + \frac{4\varrho I}{ab} \sum_{k=1}^{\infty}\sum_{l=1}^{\infty} \frac{\left(\begin{array}{c} \cos\frac{k\pi}{a}x_{in}\ \cos\frac{l\pi}{b}y_{in} \frac{\sin\left(\frac{k\pi}{a}\frac{h_{xin}}{2}\right)}{\frac{k\pi}{a}\frac{h_{xin}}{2}} \frac{\sin\left(\frac{l\pi}{b}\frac{h_{yin}}{2}\right)}{\frac{l\pi}{b}\frac{h_{yin}}{2}} \\ -\cos\frac{k\pi}{a}x_{out}\ \cos\frac{l\pi}{b}y_{out} \frac{\sin\left(\frac{k\pi}{a}\frac{h_{xout}}{2}\right)}{\frac{k\pi}{a}\frac{h_{xout}}{2}} \frac{\sin\left(\frac{l\pi}{b}\frac{h_{yout}}{2}\right)}{\frac{l\pi}{b}\frac{h_{yout}}{2}} \end{array}\right)}{\sinh\left(c\sqrt{\left(\frac{k\pi}{a}\right)^2 + \left(\frac{l\pi}{b}\right)^2}\right)\sqrt{\left(\frac{k\pi}{a}\right)^2 + \left(\frac{l\pi}{b}\right)^2}} \\ & \times \cos\frac{k\pi}{a}x \cos\frac{l\pi}{b}y \cosh\left(\sqrt{\left(\frac{k\pi}{a}\right)^2 + \left(\frac{l\pi}{b}\right)^2}(z-c)\right) \end{aligned} \tag{47}$$

Shrinking the rectangle's dimensions h_{xin} and h_{yin} with center point $s = (x_{in}, y_{in})$ to zero, re-establishes the point injection at (x_{in}, y_{in}) and the voltage (47) reduces to (10). The modified resistance $R_{sd} = \frac{V(x_{in},y_{in},0)-V(x_{out},y_{out},0)}{I}$, with rectangular current in- and ejection area centered around the source s and drain d, respectively, and lying entirely within the beam's faces, is

$$R'_{sd} = \frac{4\varrho}{ab}\sum_{k=0}^{\infty}\sum_{l=0}^{\infty}\gamma_{kl}\frac{\left(\begin{array}{c}\cos\frac{k\pi}{a}x_{in}\ \cos\frac{l\pi}{b}y_{in}\frac{\sin\left(\frac{k\pi}{a}\frac{h_{xin}}{2}\right)}{\frac{k\pi}{a}\frac{h_{xin}}{2}}\frac{\sin\left(\frac{l\pi}{b}\frac{h_{yin}}{2}\right)}{\frac{l\pi}{b}\frac{h_{yin}}{2}}\\ -\cos\frac{k\pi}{a}x_{out}\ \cos\frac{l\pi}{b}y_{out}\frac{\sin\left(\frac{k\pi}{a}\frac{h_{xout}}{2}\right)}{\frac{k\pi}{a}\frac{h_{xout}}{2}}\frac{\sin\left(\frac{l\pi}{b}\frac{h_{yout}}{2}\right)}{\frac{l\pi}{b}\frac{h_{yout}}{2}}\end{array}\right)^2}{\sqrt{\left(\frac{k\pi}{a}\right)^2+\left(\frac{l\pi}{b}\right)^2}}\coth\left(c\sqrt{\left(\frac{k\pi}{a}\right)^2+\left(\frac{l\pi}{b}\right)^2}\right) \tag{48}$$

For sufficiently large k and l, the double sum in (48) tends to

$$S'_{3D} \simeq \frac{4\varrho}{ab}\sum_{k=K_k}^{\infty}\sum_{l=K_k}^{\infty}\frac{\left(\cos\frac{k\pi}{a}x_{in}\cos\frac{l\pi}{b}y_{in}\frac{\sin\left(\frac{k\pi}{a}\frac{h_{xin}}{2}\right)}{\frac{h_{xin}}{2}}\frac{\sin\left(\frac{l\pi}{b}\frac{h_{yin}}{2}\right)}{\frac{h_{yin}}{2}}-\cos\frac{k\pi}{a}x_{out}\cos\frac{l\pi}{b}y_{out}\frac{\sin\left(\frac{k\pi}{a}\frac{h_{xout}}{2}\right)}{\frac{h_{xout}}{2}}\frac{\sin\left(\frac{l\pi}{b}\frac{h_{yout}}{2}\right)}{\frac{h_{yout}}{2}}\right)^2}{\frac{k\pi}{a}\frac{l\pi}{b}\sqrt{\left(\frac{k\pi}{a}\right)^2+\left(\frac{l\pi}{b}\right)^2}}$$

which always converges for all involved *positive* parameters, because both sums are convergent series of the type $\sum_{n=K_n}^{\infty}\frac{1}{n^{1+\varepsilon}}$ with $\varepsilon > 0$. Taking the limit $c \to 0$ combined with the renormalization $\frac{\varrho I}{c} = 1$ transforms the 3D voltage (47) with rectangular current in- and ejection as well as the corresponding resistance (48) to the 2D analogon (whose Fourier equations are also verified to convergence always for positive rectangle sizes $h_{xin} > 0$, $h_{yin} > 0$, $h_{xout} > 0$ and $h_{yout} > 0$.)

In spite of the mathematical elegant modeling of point in- and ejection, caution is always required to deduce conclusions beyond the (sometimes implicitly made) modeling assumptions.

F The function $w(z, A)$ in (37) and q-analysis

We deduce properties of the function $w(z, A)$, defined by the series

$$w(z, A) = \sum_{n=1}^{\infty}\frac{z^n}{n\sinh(An)}$$

in (37). Provided that $A \neq 0$, the series $\sum_{n=1}^{\infty}\frac{z^n}{n\sinh(An)}$ in (37) converges for $\left|ze^{-A}\right| < 1$. Indeed, the absolute value is

$$|w(z, A)| \leq 2\sum_{n=1}^{\infty}\frac{|z|^n}{n\left|e^{An}-e^{-An}\right|} = 2\sum_{n=1}^{\infty}\frac{\left|ze^{-A}\right|^n}{n\left|1-e^{-2An}\right|}$$

Since $\left|1-e^{-2A}\right| < \left|1-e^{-2An}\right| \leq 1$ for all integer $n > 0$, we conclude, for $\left|ze^{-A}\right| < 1$, that

$$|w(z, A)| \leq \frac{-2\log\left(1-\left|ze^{-A}\right|\right)}{|1-e^{-2A}|}$$

We rewrite (37) as

$$w(z, A) = 2\sum_{n=1}^{\infty}\frac{\left(ze^{-A}\right)^n}{n\left(1-e^{-2An}\right)} = 2\sum_{n=1}^{\infty}\sum_{k=0}^{\infty}\left(e^{-2An}\right)^k\frac{\left(ze^{-A}\right)^n}{n}$$

We can reverse the sums due to absolute convergence,

$$w\left(z,A\right)=2\sum_{k=0}^{\infty}\sum_{n=1}^{\infty}\frac{\left(ze^{-A(1+2k)}\right)^{n}}{n}=-2\sum_{k=0}^{\infty}\log\left(1-ze^{-A(1+2k)}\right)=-2\log\prod_{k=0}^{\infty}\left(1-ze^{-A(1+2k)}\right)$$

Hence, for $\left|ze^{-A}\right|<1$, we find that

$$\begin{aligned}w\left(z,A\right)&=\sum_{n=1}^{\infty}\frac{z^{n}}{n\sinh\left(An\right)}=-2\sum_{k=0}^{\infty}\log\left(1-ze^{-A(1+2k)}\right)\\&=-2\log\left(1-ze^{-A}\right)-2\log\left(1-ze^{-3A}\right)-2\log\left(1-ze^{-5A}\right)+\cdots\end{aligned}\tag{49}$$

The definition (37) of $w\left(z,A\right)=2\sum_{n=1}^{\infty}\frac{z^{n}}{n(e^{An}-e^{-An})}$, for $|z|<1$, indicates that

$$w\left(ze^{A},A\right)-w\left(ze^{-A},A\right)=2\sum_{n=1}^{\infty}\frac{z^{n}\left(e^{An}-e^{-An}\right)}{n\left(e^{An}-e^{-An}\right)}=2\sum_{n=1}^{\infty}\frac{z^{n}}{n}$$

from which we obtain

$$w\left(ze^{A},A\right)-w\left(ze^{-A},A\right)=-2\log\left(1-z\right)$$

Replace $x=ze^{A}$, then $z=e^{-A}x$ and $w\left(x,A\right)=-2\log\left(1-e^{-A}x\right)+w\left(xe^{-2A},A\right)$. Writing again z for x, results in the recursion

$$w\left(z,A\right)=-2\log\left(1-e^{-A}z\right)+w\left(ze^{-2A},A\right)\tag{50}$$

After p iterations of the recursion (50), we find that

$$w\left(z,A\right)=-2\sum_{k=0}^{p}\log\left(1-ze^{-A(1+2k)}\right)+w\left(ze^{-2pA},A\right)\tag{51}$$

Since e^{-2pA} rapidly tends to zero if p increases and $w\left(0,A\right)=0$, the p-th iteration (51) leads again to (49) in the limit $p\to\infty$. In other words, the recursion (50) allows us to write the sum in $w\left(z,A\right)$ up to any desired accuracy.

Interestingly, the product in $w\left(z,A\right)=-2\log\left(\prod_{k=0}^{\infty}\left(1-ze^{-A(1+2k)}\right)\right)$ is written, with $q=e^{-2A}$, as

$$\prod_{k=0}^{\infty}\left(1-ze^{-A(1+2k)}\right)=\prod_{k=0}^{\infty}\left(1-ze^{-A}q^{k}\right)=\left(ze^{-A};q\right)_{\infty}$$

where

$$\left(a;q\right)_{n}=\prod_{k=0}^{n-1}\left(1-aq^{k}\right)$$

is known as the q-Pochhammer symbol, with $\left(a;q\right)_{0}=1$. Then, with $q=e^{-2A}$, we have

$$w\left(z,A\right)=-2\log\prod_{k=0}^{\infty}\left(1-ze^{-A}q^{k}\right)=-2\log\left(z\sqrt{q};q\right)_{\infty}\tag{52}$$

Invoking $\prod_{m=0}^{\infty}(1+q^{m}\,z)=\sum_{m=0}^{\infty}\frac{q^{m(m-1)/2}}{\prod_{j=1}^{m}(1-q^{j})}\,z^{m}$ in (60) shows, with $q=e^{-2A}$, that

$$\prod_{k=0}^{\infty}\left(1-ze^{-A}q^{k}\right)=\sum_{m=0}^{\infty}\frac{q^{\frac{m^{2}}{2}}}{\prod_{j=1}^{m}(1-q^{j})}\,\left(-z\right)^{m}\tag{53}$$

Hence, the product in (52) is

$$\prod_{k=0}^{\infty}\left(1-ze^{-A}q^k\right)=\sum_{m=0}^{\infty}\frac{e^{-Am^2}}{\prod_{j=1}^{m}(1-e^{-2Aj})}\,(-z)^m$$
$$=1-\frac{e^{-A}}{1-e^{-2A}}\,z+\frac{e^{-4A}}{(1-e^{-2A})(1-e^{-4A})}\,z^2+\sum_{m=3}^{\infty}\frac{e^{-Am^2}}{\prod_{j=1}^{m}(1-e^{-2Aj})}\,(-z)^m$$

In our setting $q=e^{-2A}=e^{-2\pi\frac{b}{a}}$ is, for a square where $a=b$, equal to $q=e^{-2\pi}=\frac{1}{535.491}\approx 2.10^{-3}$ and $e^{-A}=e^{-\pi}\approx 4.10^{-2}$, which illustrates that the series (53) converges very fast, implying that only a few terms are sufficient for numerical computations. Thus, for $q=e^{-2A}$, the product form (52) of $w\left(z,A\right)$

$$w\left(z,A\right)=-2\log\prod_{k=0}^{\infty}\left(1-ze^{-A}q^k\right)$$
$$\simeq-2\log\left(1-\frac{e^{-A}}{1-e^{-2A}}\,z+\sum_{m=2}^{K}\frac{e^{-Am^2}}{\prod_{j=1}^{m}(1-e^{-2Aj})}\,(-z)^m\right)$$

already yields a very good accuracy for a small integer $K\approx 5$, provided A is not too small.

The function (37)

$$w\left(z,A\right)=2\sum_{n=1}^{\infty}\frac{z^n}{n\left(e^{An}-e^{-An}\right)}=2\sum_{n=1}^{\infty}\frac{\left(ze^{A}\right)^n}{n\left(e^{2An}-1\right)}$$

for small A is computed with the Bernoulli expansion [10, Appendix], valid for $|t|<2\pi$,

$$\frac{1}{e^t-1}=\frac{1}{t}-\frac{1}{2}+\sum_{m=1}^{\infty}B_{2m}\,\frac{t^{2m-1}}{(2m)!}\tag{54}$$

where B_n is the n-th Bernoulli number, as

$$w\left(z,A\right)=2\sum_{n=1}^{\infty}\frac{\left(ze^{A}\right)^n}{n\left(e^{2An}-1\right)}$$
$$=2\lim_{N\to\infty}\sum_{n=1}^{N}\frac{\left(ze^{A}\right)^n}{n}\left(\frac{1}{2An}-\frac{1}{2}+\sum_{m=1}^{\infty}B_{2m}\,\frac{(2An)^{2m-1}}{(2m)!}\right)$$

Assuming that $A<\frac{\pi}{N}$, reversal of n- and m-sum shows that

$$w\left(z,A\right)=\lim_{N\to\infty}\left(\frac{1}{A}\sum_{n=1}^{N}\frac{\left(ze^{A}\right)^n}{n^2}-\sum_{n=1}^{N}\frac{\left(ze^{A}\right)^n}{n}+2\sum_{m=1}^{\infty}B_{2m}\,\frac{(2A)^{2m-1}\sum_{n=1}^{N}\frac{\left(ze^{A}\right)^n}{n^{2(1-m)}}}{(2m)!}\right)$$
$$=\lim_{N\to\infty}\left(\frac{1}{A}\sum_{n=1}^{N}\frac{\left(ze^{A}\right)^n}{n^2}-\sum_{n=1}^{N}\frac{\left(ze^{A}\right)^n}{n}+O\left(A\right)\right)$$

Since the two remaining sums exist for $N\to\infty$ and

$$\sum_{n=1}^{\infty}\frac{x^n}{n^2}=\int_0^x\sum_{n=1}^{\infty}\frac{u^{n-1}}{n}du=-\int_0^x\log\left(1-u\right)\frac{du}{u}=\int_0^{-\log(1-x)}\frac{t}{e^t-1}dt$$

we arrive, for small $A\to 0$ and $\left|ze^{A}\right|<1$, at

$$w\left(z,A\right)=\frac{1}{A}\int_0^{-\log(1-z)}\frac{t}{e^t-1}dt+\log\left(1-z\right)+O\left(A\right)$$

where the first term clearly dominates.

G Gaussian polynomials

G.1 Definition

The Gaussian polynomial for $k \geq 0$ and $l > 0$ is defined [18, pp. 250] as

$$\left[\begin{array}{c} k \\ l \end{array} \right](q) = \frac{(1-q^k)(1-q^{k-1})\cdots(1-q^{k-l+1})}{(1-q)(1-q^2)\cdots(1-q^l)} = \frac{\prod_{j=k-l+1}^{k}(1-q^j)}{\prod_{j=1}^{l}(1-q^j)} = \prod_{j=1}^{l}\frac{(1-q^{k-j+1})}{(1-q^j)} \tag{55}$$

$$= \frac{\prod_{j=1}^{k}(1-q^j)}{\prod_{j=1}^{l}(1-q^j)\ \prod_{j=1}^{k-l}(1-q^j)} \tag{56}$$

with $\left[\begin{array}{c} 0 \\ l \end{array} \right](q) = \delta_{0l}$, $\left[\begin{array}{c} k \\ 0 \end{array} \right](q) = 1$ and $\left[\begin{array}{c} k \\ -l \end{array} \right](q) = 0$. Obviously, it holds that $\left[\begin{array}{c} k \\ l \end{array} \right](0) = 1$. We list some Gaussian polynomials,

$$\left[\begin{array}{c} 3 \\ 2 \end{array} \right](q) = 1 + q + q^2$$

$$\left[\begin{array}{c} 4 \\ 2 \end{array} \right](q) = 1 + q + 2\,q^2 + q^3 + q^4$$

$$\left[\begin{array}{c} 5 \\ 2 \end{array} \right](q) = 1 + q + 2\,q^2 + 2\,q^3 + 2\,q^4 + q^5 + q^6$$

The Gaussian polynomials (55) are particularly interesting due to their intimate relation to the binomial coefficients, exemplified by the form of (56) and by

$$\left[\begin{array}{c} k \\ l \end{array} \right](1) = \binom{k}{l} \tag{57}$$

Indeed,

$$\lim_{q\to 1}\left[\begin{array}{c} k \\ l \end{array} \right](q) = \lim_{q\to 1}\prod_{j=1}^{l}\frac{(1-q^{k-j+1})}{(1-q^j)} = \prod_{j=1}^{l}\lim_{q\to 1}\frac{(1-q^{k-j+1})}{(1-q^j)} = \prod_{j=1}^{l}\frac{(k-j+1)}{j}$$

$$= \frac{1}{l!}\frac{\prod_{j=1}^{k}(k-j+1)}{\prod_{j=l+1}^{k}(k-j+1)} = \frac{1}{l!}\frac{\prod_{r=1}^{k} r}{\prod_{r=k-l}^{1} r} = \frac{k!}{l!\,(k-l)!} = \binom{k}{l}$$

The same argument shows that

$$\lim_{q\to 1}\prod_{j=0}^{n-1}\frac{(1-q^{x+j})}{(1-q)} = \prod_{j=0}^{n-1}(x+j) = \frac{\Gamma(x+n)}{\Gamma(x)} = (x)_n$$

suggesting, with the notation $(a;q)_n = \prod_{k=0}^{n-1}\left(1-aq^k\right)$, that $\frac{(q^x;q)_n}{(1-q)^n}$ is the q-extension of the Pochhammer symbol $(x)_n$.

The other important limit, for $|q| < 1$, is

$$\lim_{k\to\infty}\left[\begin{array}{c} k \\ l \end{array} \right](q) = \frac{1}{\prod_{j=1}^{l}(1-q^j)} \qquad (|q| < 1) \tag{58}$$

which directly follows, for finite l, from $\left[\begin{array}{c} k \\ l \end{array} \right](q) = \frac{\prod_{j=1}^{k}(1-q^j)}{\prod_{j=1}^{l}(1-q^j)\ \prod_{j=1}^{k-l}(1-q^j)}$.

We will demonstrate that many of the well-known relations involving binomial coefficients readily follow as special cases (i.e. evaluations at $q = 1$) of the more general results based on Gaussian polynomials. Combinatorial results based on Gaussian polynomials are discussed by Goulden and Jackson [19].

G.2 Generating function for the Gaussian Polynomials

The fundamental cornerstone in the theory of Gaussian polynomials is

$$Q_k(z,x) = \prod_{m=0}^{k-1}(x + q^m\, z) = \sum_{m=0}^{k} \left[\begin{array}{c} k \\ m \end{array} \right](q)\ q^{m(m-1)/2}\, z^m\, x^{k-m} \tag{59}$$

which bears a striking resemblance to Newton's binomium [19, 18]; see also [20, Chapter 2, Sec. 3.3]. We define $Q_k(-x,x) = \delta_{0k}$ in correspondence to the first factor for $m = 0$ in the product. Relation (59) is derived via induction from the recursion $Q_k(z,x) = (x + q^{k-1}\, z)\, Q_{k-1}(z,x)$ for $k > 0$ and $Q_0(x,z) = 1$.

When k tends to infinity, (59) leads for $|q| < 1$ with (58) to

$$\prod_{m=0}^{\infty}(1 + q^m\, z) = \sum_{m=0}^{\infty} \frac{q^{m(m-1)/2}}{\prod_{j=1}^{m}(1-q^j)}\, z^m \tag{60}$$

This relation immediately leads to two formulas due to Euler [21, sec. 19.5]. There is wealth of nice properties of the product $(a;q)_n = \prod_{k=0}^{n-1}\left(1 - aq^k\right)$. The finite product can be treated by the infinite variant as

$$\begin{aligned}(a;q)_n &= \prod_{k=0}^{n-1}\left(1 - aq^k\right) = \frac{\prod_{k=0}^{n-1}\left(1 - aq^k\right)\prod_{k=n}^{\infty}\left(1 - aq^k\right)}{\prod_{k=n}^{\infty}\left(1 - aq^k\right)} \\ &= \frac{\prod_{k=0}^{\infty}\left(1 - aq^k\right)}{\prod_{k=0}^{\infty}\left(1 - aq^{k+n}\right)} = \frac{(a;q)_\infty}{(aq^n;q)_\infty}\end{aligned}$$

We add the important relation of Gaussian polynomials

$$\prod_{j=1}^{n}(1 + z\, q^{2j-1})(1 + z^{-1}\, q^{2j-1}) = \sum_{k=-n}^{n} \left[\begin{array}{c} 2n \\ n+k \end{array} \right](q^2)\ q^{k^2}\, z^k \tag{61}$$

which is a finite version of famous Jacobi's triple product[13] [21, sec. 19.8],

$$\theta_3(z,q) = \sum_{k=-\infty}^{\infty} z^k\, q^{k^2} = \prod_{m=1}^{\infty}\left(1 - q^{2m}\right)\left(1 + z\, q^{2m-1}\right)\left(1 + z^{-1}\, q^{2m-1}\right) \tag{63}$$

that illustrates the intimate connection of the product $(a;q)_n = \prod_{k=0}^{n-1}\left(1 - aq^k\right)$ and elliptic functions!

We must refer to the large literature (see e.g. [19, 18, 22, 20]) on the product $(a;q)_n = \prod_{k=0}^{n-1}\left(1 - aq^k\right)$.

[13] There seems to exist a large variety of such identities. Another is Watson's quintuple product

$$\sum_{k=-\infty}^{\infty}(z^{3k} - z^{-3k-1})\, q^{k(3k+2)/2} = \prod_{m=1}^{\infty}(1-q^m)\,(1 - z\, q^m)\left(1 - z^{-1}\, q^{m-1}\right)\left(1 - z^2\, q^{2m-1}\right)\left(1 - z^{-2}\, q^{2m-1}\right) \tag{62}$$

G.3 Examples of q-extension

G.3.1 The q-Gamma function

The q-Gamma function is defined by

$$\Gamma_q(x) = (1-q)^{1-x} \frac{(q;q)_\infty}{(q^x;q)_\infty} = (1-q)^{1-x} \frac{\prod_{k=0}^{\infty}\left(1-q^{k+1}\right)}{\prod_{k=0}^{\infty}\left(1-q^{k+x}\right)} = (1-q)^{1-x} \prod_{k=0}^{\infty} \frac{\left(1-q^{k+1}\right)}{\left(1-q^{k+x}\right)} \tag{64}$$

Explicitly,

$$\Gamma_q(x) = (1-q)^{1-x} \lim_{m\to\infty} \frac{(1-q)}{(1-q^x)} \frac{\left(1-q^2\right)}{\left(1-q^{1+x}\right)} \frac{\left(1-q^3\right)}{\left(1-q^{2+x}\right)} \cdots \frac{\left(1-q^{m+1}\right)}{\left(1-q^{m+x}\right)}$$

If $x = n \in \mathbb{N}$, then

$$\begin{aligned}\Gamma_q(n) &= (1-q)^{1-n} \frac{\prod_{k=0}^{\infty}\left(1-q^{k+1}\right)}{\prod_{k=0}^{\infty}\left(1-q^{k+n}\right)} = (1-q)^{1-n} \frac{\prod_{k=1}^{\infty}\left(1-q^{k}\right)}{\prod_{k=n}^{\infty}\left(1-q^{k}\right)} \\ &= (1-q)^{1-n} \prod_{k=1}^{n-1}\left(1-q^k\right) = \prod_{k=1}^{n-1} \frac{1-q^k}{1-q}\end{aligned}$$

and

$$\lim_{q\to 1} \Gamma_q(n) = \prod_{k=1}^{n-1} \frac{1-q^k}{1-q} = \prod_{k=1}^{n-1} \lim_{q\to 1} \frac{1-q^k}{1-q} = \prod_{k=1}^{n-1} k = (n-1)! = \Gamma(n)$$

The q-Gamma function satisfies the functional equation

$$\Gamma_q(x+1) = \frac{1-q^x}{1-q}\Gamma_q(x) \tag{65}$$

Indeed, the definition (64) indicates that

$$\begin{aligned}\frac{\Gamma_q(x+1)}{\Gamma_q(x)} &= \frac{1}{1-q} \prod_{k=0}^{\infty} \frac{\left(1-q^{k+x}\right)}{\left(1-q^{k+x+1}\right)} = \frac{1}{1-q} \frac{\prod_{k=0}^{\infty}\left(1-q^{k+x}\right)}{\prod_{k=0}^{\infty}\left(1-q^{k+x+1}\right)} \\ &= \frac{1}{1-q} \frac{\prod_{k=0}^{\infty}\left(1-q^{k+x}\right)}{\prod_{k=1}^{\infty}\left(1-q^{k+x}\right)} = \frac{1}{1-q}\left(1-q^{k+x}\right)\end{aligned}$$

which is the functional equation (65). After the limit $q \to 1$ in the functional equation (65), we arrive, with $\Gamma_1(x) = \Gamma(x)$, at the functional equation $\Gamma(x+1) = x\Gamma(x)$ of the Gamma function.

We follow Gosper's trick in [22, Appendix A], who was inspired by Gauss' deduction of the Euler-Gauss product of the Gamma function [10, Part II]

$$\Gamma(z+1) = \prod_{n=1}^{\infty} \left(1+\frac{1}{n}\right)^z \left(1+\frac{z}{n}\right)^{-1} \tag{66}$$

in inserting

$$(1-q)^x = \frac{\prod_{k=0}^{\infty}\left(1-q^{k+1}\right)^x}{\prod_{k=1}^{\infty}\left(1-q^{k+1}\right)^x} = \prod_{k=1}^{\infty}\left(\frac{1-q^k}{1-q^{k+1}}\right)^x$$

in (64) to obtain

$$\begin{aligned}\Gamma_q(x+1) &= (1-q)^{-x} \prod_{k=0}^{\infty} \frac{\left(1-q^{k+1}\right)}{\left(1-q^{k+x+1}\right)} = \prod_{k=1}^{\infty}\left(\frac{1-q^{k+1}}{1-q^k}\right)^x \prod_{k=1}^{\infty} \frac{\left(1-q^k\right)}{\left(1-q^{k+x}\right)} \\ &= \prod_{k=1}^{\infty}\left(\frac{1-q^k+q^k-q^{k+1}}{1-q^k}\right)^x \left(\frac{1-q^k}{1-q^{k+x}}\right)\end{aligned}$$

Further, with $\frac{1-q^{k+1}}{1-q^k} = \frac{1-q^k+q^k-q^{k+1}}{1-q^k} = 1 + q^k \frac{1-q}{1-q^k}$ and $\frac{1-q^k}{1-q^{k+x}} = \left(\frac{1-q^{k+x}}{1-q^k}\right)^{-1} = \left(\frac{1-q^k+q^k-q^{k+x}}{1-q^k}\right)^{-1} = \left(1 + q^k \frac{1-q^x}{1-q^k}\right)^{-1}$, we find the q-extension of the Euler-Gauss product,

$$\Gamma_q(x+1) = \prod_{k=1}^{\infty} \left(1 + q^k \frac{1-q}{1-q^k}\right)^x \left(1 + q^k \frac{1-q^x}{1-q^k}\right)^{-1} \tag{67}$$

Immediately, the limit $q \to 1$ reduces to the Euler-Gauss product (66).

G.3.2 The q-sinus

We compute with (67) the product

$$\begin{aligned}
\Gamma_q(1+x)\Gamma_q(1-x) &= \prod_{k=1}^{\infty} \left(1 + q^k \frac{1-q^x}{1-q^k}\right)^{-1} \left(1 + q^k \frac{1-q^{-x}}{1-q^k}\right)^{-1} \\
&= \prod_{k=1}^{\infty} \frac{1-q^k}{1-q^{k+x}} \frac{1-q^k}{1-q^{k-x}} = \prod_{k=1}^{\infty} \frac{1-2q^k+q^{2k}}{1-q^k\left(q^x+q^{-x}\right)+q^{2k}} \\
&= \prod_{k=1}^{\infty} \frac{1-2q^k+q^{2k}}{1-2q^k\cosh(x\log q)+q^{2k}}
\end{aligned}$$

The infinite product of the sinus function [23, 4.3.89]

$$\frac{\sin(\pi z)}{\pi z} = \prod_{k=1}^{\infty} \left(1 - \frac{z^2}{k^2}\right) \tag{68}$$

then suggests that

$$\lim_{q\to 1} \prod_{k=1}^{\infty} \frac{1-q^k}{1-q^{k+x}} \frac{1-q^k}{1-q^{k-x}} = \prod_{k=1}^{\infty} \frac{k^2}{(k+x)(k-x)} = \prod_{k=1}^{\infty} \frac{1}{\left(1-\frac{x^2}{k^2}\right)} = \frac{\pi x}{\sin(\pi x)}$$

Since $\Gamma_q(1+x)\Gamma_q(1-x) = \frac{1-q^x}{1-q}\Gamma_q(x)\Gamma_q(1-x)$ is, by q-definition, equal to $\Gamma_q(x)\Gamma_q(1-x) = \frac{\pi}{\sin_q(\pi x)}$, so that we may conclude that

$$\Gamma_q(1+x)\Gamma_q(1-x) = \frac{1-q^x}{1-q}\Gamma_q(x)\Gamma_q(1-x) = \frac{1-q^x}{1-q}\frac{\pi}{\sin_q(\pi x)} = \prod_{k=1}^{\infty} \frac{1-q^k}{1-q^{k+x}} \frac{1-q^k}{1-q^{k-x}}$$

Hence, the q-extension of the sinus product (68) is

$$\sin_q(\pi x) = \pi \frac{1-q^x}{1-q} \prod_{k=1}^{\infty} \frac{1-q^{k+x}}{1-q^k} \frac{1-q^{k-x}}{1-q^k}$$